27
6/17/77
25 cys to NTIS

UCID- 17435

Lawrence Livermore Laboratory

A DEVICE FOR MEASURING THE ION ANGULAR DISTRIBUTION OF 2XIIB PLASMA

Bruce Smith

April 6, 1977

This is an informal report intended primarily for internal or limited external distribution. The opinions and conclusions stated are those of the author and may or may not be those of the laboratory.

Prepared for U.S. Energy Research & Development Administration under contract No. W-7405-Eng-48.

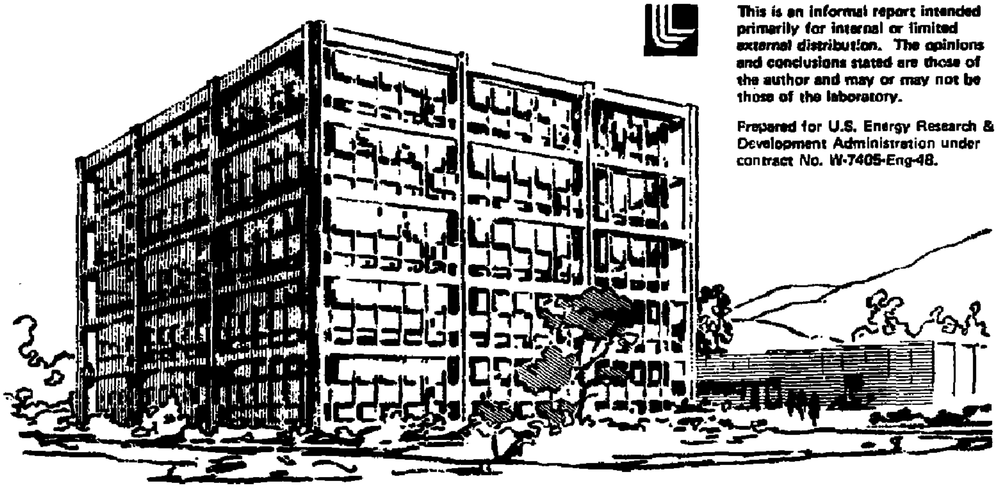

MASTER

DISTRIBUTION OF THIS DOCUMENT IS UNLIMITED

CONTENTS

A DEVICE FOR MEASURING THE ION ANGULAR DISTRIBUTION OF 2XIIB PLASMA

ABSTRACT

This paper describes a device that measures charge-exchange flux to determine the angular distribution of the 2XIIB plasma. Charge-exchange products heat circular nickel foils (placed at 15° intervals in θ and at constant radius on an arc parallel to the z-axis) and the voltage drop across the foils (produced by constant-current sources) provides a measure of the changes in resistivity. The charge-exchange flux at each foil is proportional to the plasma distribution at that angle. Use of this technique is limited by the resistivity and heat resistance of the circular nickel foils, but could conceivably be extended to other shapes and materials. We compare Hall-Simonen[1] and "time-average" measurement of angular distribution and calculate characteristic times of loss (gain) from theory. The $g(\mu)$ detector may be used to experimentally verify these times of loss (gain) and also to analyze plasma pressure stability. Current microwave measurements show that plasma has an exponential density dependence in z and assumes a flux tube rather than a $p(B)$ density dependence. A distinct angular distribution (determinable by the detector) is associated with each of these dependencies. We also discuss codes to simulate injection and resulting angular distribution, charge-exchange capture, and heating and signal of the detectors.

INTRODUCTION

Determination of plasma angular distribution in the 2XIIB machine is a matter of considerable interest. This measurement, when properly interpreted, may aid in the evaluation of such plasma parameters as stability, well depth, plasma shape, energy distribution, and evolution of plasma in velocity space. Angular distribution of the plasma had previously been evaluated only from microwave measurement of axial plasma densities.[1,2] However, this evaluation involves assumptions about plasma shape (flux tube or $p(B)$?); and microwave density measurements do not differentiate between "hot" and "cold" plasma components.

Measurement of charge-exchange products from within the plasma offers an alternative means for determining angular distribution. Background-gas or beam neutrals exchange electrons with ions and the resulting energetic neutrals (formerly plasma ions) continue on with the same $\overline{v}$ as the original ion.

If we know the distribution of neutrals and ions within the plasma, we may directly determine the charge-exchange reaction rate

$$R \equiv \text{reaction rate} = A \iiint f(\overline{v}_i) f(\overline{v}_n)\ |\overline{v}|\ \sigma\ (|\overline{v}|)\ d^3\,\overline{v}_i\ d^3\,\overline{v}_n\ dV$$

where "i" refers to the ions, "n" refers to the neutrals, $\overline{v} \equiv \overline{v}_n - \overline{v}_i$, $\sigma(|v|)$ is the charge-exchange cross section, and A is the normalization constant. Assuming $f(\overline{v}_i)$ is separable into $f(v_i,\ \phi_i)\ g(\mu)$ where $\mu = \cos\theta$ and taking $|\overline{v}|$ as constant, we may determine the angular distribution of the plasma in a small volume element $dV = d^3 r_i$:

$$R \propto \iint g(\mu)\ \sin\theta\ d\ \theta\ dV\ .$$

In the limit $dV \to 0$, $g(\mu)$ is independent of r_i so that

$$R \propto \int g(\mu)\ d\mu$$

and

$$g(\mu) \propto dR/d\mu\ .$$

If we center a large sphere on volume element dV (Fig. 1), the average flux of particles at the surface of the sphere will equal the reaction rate divided by the surface area so that

$$\langle\Phi\rangle = R/4\pi\ r_0^2\ \text{neutrals/cm}^2\text{s}\ \ (r_0 \equiv \text{radius of the sphere}).$$

The reaction rate may then be redefined as

$$R = 4\pi\ r_0^2\ \langle\Phi\rangle\ .$$

The differential reaction rate $(dR/d\theta)$ may be obtained by observing that the neutrals for small dV strike the surface of the enclosing sphere with the same distribution $g(\mu)$ as they do for the velocity $(\Phi = \langle\Phi\rangle g(\mu))$, so that for a differential element of area dA $(r_0 \sin\theta\ d\phi)\ (r_0\ d\theta)$

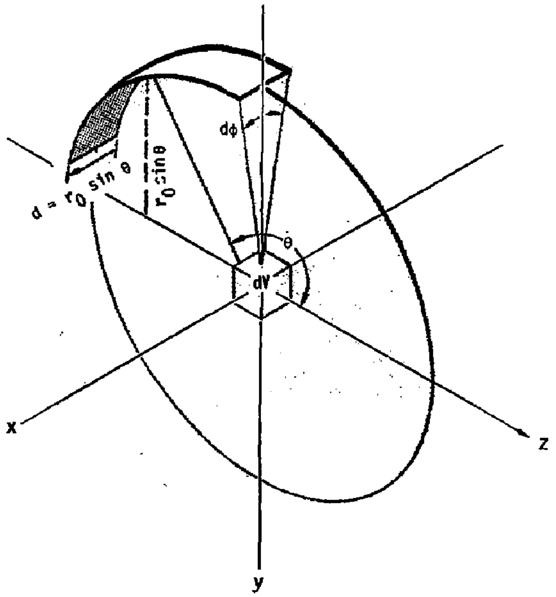

Fig. 1. Flux sphere.

$$\int dR = 4\pi\, r_0^2 \frac{\int \Phi(\theta)\, dA}{\int dA} = \langle\Phi\rangle \int g(\mu)\ (r_0 \sin\theta\, d\phi)\ (r_0\, d\theta)$$

and

$$dR = \langle\Phi\rangle\ g(\mu)\ (r_0 \sin\theta\, d\phi)\ (r_0\, d\theta)\ .$$

Let us now require that $r_0 \sin\theta\, d\phi$ be constant so that the "width" of dA across the z axis is constant for varying θ. Then

$$dR = g(\mu)\ \langle\Phi\rangle\ r_0\, d\theta\, d\ \ (d \equiv r_0 \sin\theta\, d\phi)$$

and

$$g(\mu) \propto dR/d\theta \propto d\Phi/d\theta\ .$$

We can measure $g(\mu)$ directly by detecting the local magnitudes of flux at small area elements (dA) as a function of angular position.

DESCRIPTION OF EXPERIMENT

The $g(\mu)$ detector measures plasma angular distribution from charge-exchange flux in the 2XIIB. Five stainless-steel tubes are mounted at a radius of 13 in. from the plasma center in a plane of constant $\phi = \arctan(y/x)$. The tubes are oriented along lines of constant $\theta = \arcsin v_\perp/|v|$ at 15° intervals from 90-150°. The positive z-axis defines both the mirror center line and $\theta = 0°$ (Fig. 2).

Each tube is 4 in. long and 0.43 in. in diameter. At the end of each tube (13-in. radius) is a thin (~0.0001-in.) nickel foil. Charge-exchange products from the plasma center enter the detectors and heat the foils. Each foil is connected to an external constant-current source by a length of coaxial cable. As the foils heat, their resistances increase. Oscilloscopes detect the changes in resistance as voltage drops across the foils. Comparison of voltage at each detector gives a direct measurement of flux at the foils; thus $g(\mu)$ may be determined.

Neutral sources for the plasma are the 50 A LBL neutral injectors, neutral-charge exchange products traversing the plasma, and neutral-background gas. Of primary concern are the 12 neutral injectors. Each injector consists

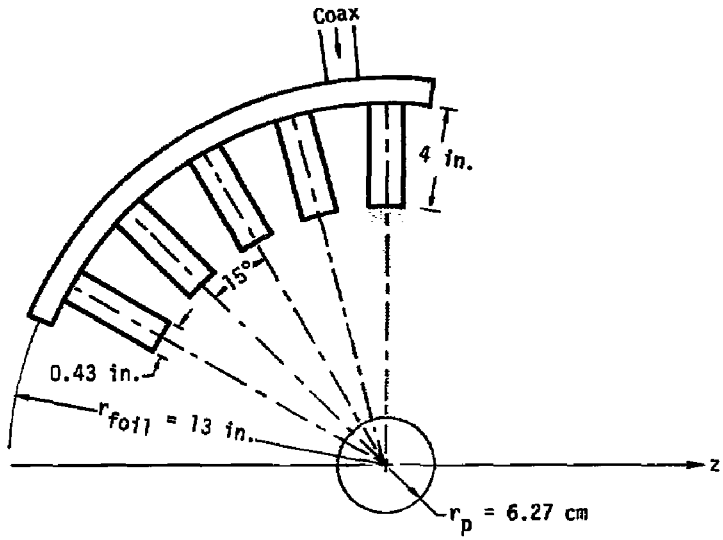

Fig. 2. Drawing of experiment.

of a 35-cm strip of beamlets all aimed at a common focus. The injectors are arranged symmetrically in a radial pattern about the z-axis at radii of 330 and 380 cm (Fig. 3). The beamlets project a rectangular pattern with

$$S = S_0 \exp\left(-\frac{\theta_z}{2^\circ}\right)^2 \exp\left(-\frac{\theta_y}{0.6^\circ}\right)^2 \frac{\text{neutrals}}{\text{s}} \text{ (Ref. 3)}$$

where S_0 is a constant source term, and θ_z and θ_y are angular deviations in θ and ϕ respectively.

The particles in the beam are deuterium atoms of $\langle E \rangle = 14.7$ keV (50% 20 keV, 40% 10 keV and 10% 6.7 keV.[4]) Background gas may be ignored because of its low density relative to the neutral-beam density. The plasma volume that concerns us is the entire plasma volume, although only a small portion of this volume is "seen" by the detectors. "Secondary" charge-exchange products may react within the volume seen despite initial interaction within an alternate volume element. The actual volume of plasma seen by the detectors may be approximated by a ball of radius $r = 6.27$ cm (Fig. 2).

Let us now approximate typical signals to be expected at each detector. Let us assume the plasma ions are stationary on the average $(\langle v_i \rangle) = 0$ so that the relative velocity (energy) of interaction is that of the neutral. Then we have

$$\langle \sigma v \rangle = \frac{dR}{n_i n_n dV} \approx 1.25 \times 10^{-7} \text{ cm}^3 \text{s}^{-1} \text{ (Ref. 5)}$$

for $\langle E_n \rangle \sim 14.7$ keV.

The source strength of the beam within the volume seen is

$$\approx \frac{S_0 \text{ (beam in volume seen)}}{\text{(beam in total volume)}}$$

$$= \frac{S_0 \int_{-6.27}^{6.27} e^{-\left(\frac{z}{12}\right)^2} dz}{\int_{\infty}^{\infty} e^{-\left(\frac{z}{12}\right)^2} dz}$$

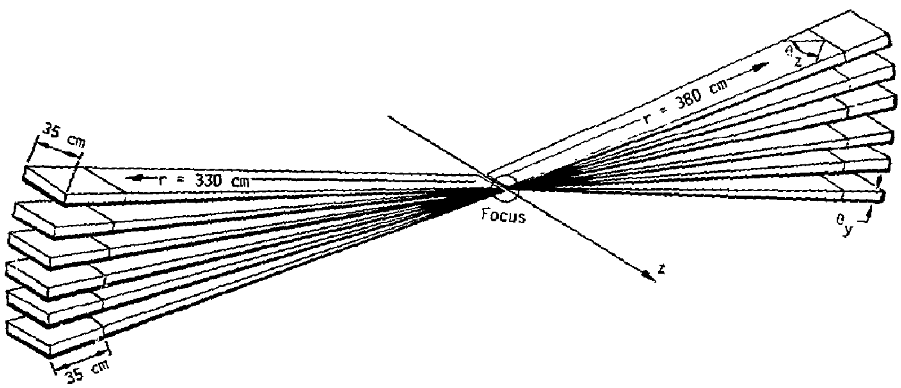

Fig. 3. Beams.

$$= S_0 \int_{-6.27}^{6.27} \left(\frac{1}{\sqrt{2\pi}}\right) e^{-1/2\left(\frac{z}{6\sqrt{2}}\right)^2}$$

$$= 0.54\ S_0$$

where we have taken the beam to be focused at $z = 0$ and have approximated $\theta_y \approx 0$ and $\theta_z/2° \approx z/12$ ($12 \approx 350 \tan 2°$).[4] For a source strength $S_0 = 330$ A we have $S \approx 180$ A.

The neutral velocity is

$$V_n = \sqrt{2\ E/m}$$

$$\approx \sqrt{2(14.7 \times 10^3\ \mathrm{eV})(1.6 \times 10^{-19}\ \mathrm{J/eV})/(2 \times 1.67 \times 10^{-27}\ \mathrm{kG})}$$

$$\approx 1.2 \times 10^6\ \mathrm{ms}^{-1}$$

$$\approx 1.2 \times 10^8\ \mathrm{cm\ s}^{-1}\ .$$

Finally, we can calculate the beam density as

$$n_n = (180\ \mathrm{C/s})/[1.6 \times 10^{-19}\ \mathrm{C/neutral} \times 1.2 \times 10^8\ \mathrm{cm\ s}^{-1} \times \pi(6.27)^2\ \mathrm{cm}^2]$$

$$= 7.6 \times 10^{10}\ \mathrm{cm}^{-3}\ .$$

Plasma parameters may typically be taken as $n \cong 1.2 \times 10^{14}\ \mathrm{cm}^{-3}$ and $\langle E \rangle \cong 9$ keV.[2] Since the charge-exchange neutral (D^2) has the same energy as its ion parent (D^{2+}), we can calculate the energy flux at the foils as

$$R = (7.6 \times 10^{10}\ D^2/\mathrm{cm}^3)(1.2 \times 10^{14}\ D^{2+}/\mathrm{cm}^3)(1.25 \times 10^{-7}\ \mathrm{cm}^3/\mathrm{s}) \times [4/3\pi(6.27)^3\ \mathrm{cm}^3]$$

$$= 1.18 \times 10^{21}\ \mathrm{s}^{-1}$$

$$= \frac{1.18 \times 10^{21}\ \mathrm{s}^{-1}}{[4\pi(13 \times 2.54)^2\ \mathrm{cm}^2]} \times (9 \times 10^3\ \mathrm{eV/particle})(1.6 \times 10^{-19}\ \mathrm{J/eV})$$

$$= 128\ \mathrm{J/cm^2\ s}$$

$= 128\ \mathrm{W/cm}^2$ for an isotropic distribution.

Assuming the total flux is stopped by the foil, we can estimate the voltage generated. The geometry of the foil is pictured in Fig. 4. The differential resistance of the foil is $d\Omega = \rho dr/A$, so that the total resistance is

$$\Omega = \int_{r_{min}}^{r_{max}} \rho\, dr/2\pi rt \qquad (\rho = \text{resistivity},\ t = \text{thickness})$$

$$= \frac{\rho}{2\pi t} \ln r \Big|_{r_{min}}^{r_{max}}$$

$$= \frac{\rho}{2\pi t} \ln \left(\frac{r_{max}}{r_{min}}\right) .$$

For $\rho_{nickel} = 6.84\ [1 + 6.9 \times 10^{-3}\ (T - 20)(°C)]\ \mu$ ohm cm, $t = 0.0001$ in., $r_{max} = 0.43$ in./2, and $r_{min} = 0.125$ in./2 we have:

$$\Omega = 0.053\ [1 + 6.9 \times 10^{-3}\ (T - 20)]\ \text{ohms.}$$

If we take the plasma duration $\tau = 10$ ms, we will have a net deposition of energy $R\tau = 1.54$ W/cm^2 or for the foil area

$$(1.28\ \text{W/cm}^2) \left[(\pi) \left(\frac{0.43\ \text{in.}}{2}\right)^2 (2.54\ \text{in./cm}^2\right] = 1.20\ \text{J}$$

The heat capacity and density of nickel are $c_p = 0.1125$ cal/g°C and $m = 8.9$ g/cm^3 so that the total temperature rise is

$$\Delta T = \frac{1.20\ \text{J}}{mV_{foil}\ c_p\ (4.18\ \text{J/cal})}$$

$$= \frac{1.20}{(8.9)[(0.43/2)^2\ \pi(0.0001)\ (2.54)^3]\ (0.1125)\ (4.18)}$$

$$= 1206.9°\text{C}^*$$

*The melting point of nickel is 1453°C so that this ΔT would probably be unacceptable. Further calculations show that, due to collimation, the flux and therefore ΔT will be much smaller (see Appendix B and C).

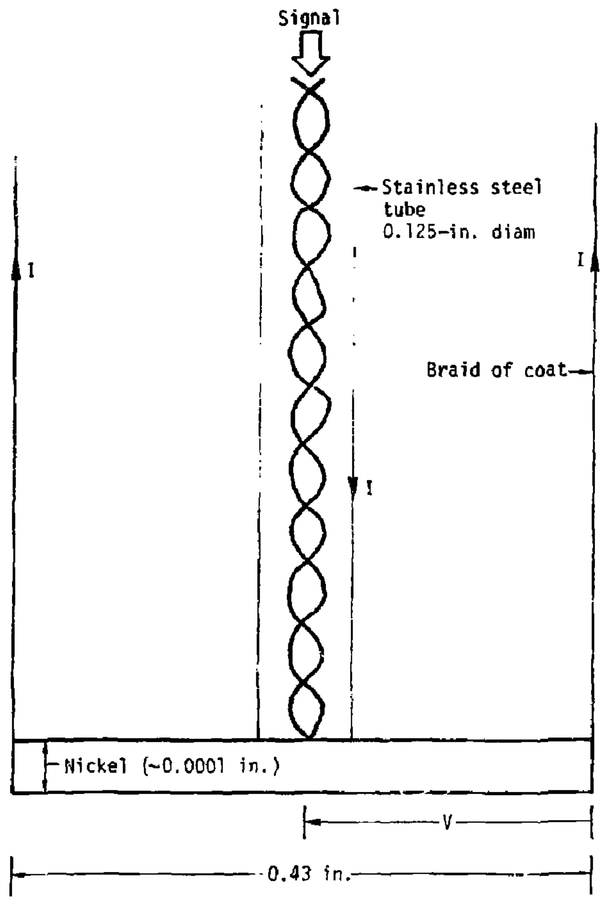

Fig. 4. Foil geometry.

for a voltage rise of $\Delta V \approx I(\Delta\Omega) \approx 494\ I$ mV ($T_0 = 20°C$). Since we are able to measure voltages of ~10 mV or less, a signal should be detectable down to ~2% of isotropic (assuming I = 1 A).

This method has peculiar constraints which prevent raising the signal to detectable levels simply by increasing the current. The foil is heated by I^2R (ohmic heating) which damps out the signal response. While results may be corrected for this damping, the current must be applied for a greater period than the plasma lifetime; and available control equipment dictates that $t_{current} \geq 0.3$ s. During this time roughly 0.3 (I^2) (0.053) J enter the foil or, for I = 10 A (1.59 J) ΔT = 1600°C. Since the melting point for nickel is 1453°C, an absolute upper limit on I (assuming constant resistivity and no heat loss) is 9.5 A. Radiation cooling of the foil at melting temperature is

$$W = e\sigma\ T^4 \quad (\sigma \equiv \text{Stefan-Boltzmann constant, } e \equiv \text{emissivity})$$

$$= (0.3)\ (5.669 \times 10^{-5})\ (T^4)\ \text{erg/s cm}^2$$

$$= 1.7 \times 10^{-5}\ T^4$$

$$= 1.7 \times 10^{-12}\ T^4\ \text{J/s cm}^2$$

$$WA \approx 14\ \text{J/s} \quad (A \equiv \text{foil area})$$

so that a more reasonable estimate is

$$I_{max} = \sqrt{W/\Omega}$$

$$= \sqrt{14/0.053}$$

$$= 16\ \text{A in steady state.}$$

In any case, the stress imposed by high temperature coupled with any $\bar{J} \times \bar{B}$ force is likely to damage the detectors.

Making the foils thicker would not solve the problem since the signal directly decreases as the thickness increases. If this technique is used in other experiments in a similar environment and these bounds are prohibitive, other foil materials or shapes must be utilized.

We have developed a code that simulates the foil signals and heating and cooling during the experiment. This allows us to vary the flux, current, and time parameters to check the above constraints, and to provide estimates of expected signals. (See App. B.)

EXPERIMENTAL ANALYSIS

If sufficient signals are available to obtain $g(\mu)$ for the plasma center, the angular distribution for the entire plasma may be determined. This angular distribution is defined as $g(\nu)$ where

$$\nu = \sin^2 \theta/B = \sin^2 \theta_0/B_{min} \; . \; (B \equiv B(z),\ \theta \equiv \theta(z)) \text{ (Ref. 1).}$$

A simple way to examine the relationship between angular distributions in z is to calculate the time spent in element dz of a field line. Let us consider a particle with pitch angle θ_0 at B_{min} of the plasma. The period of this particle is

$$T = \int_0^{z_{max}} \frac{dz}{V_{\parallel}(z)}$$

and the time in an element $\Delta z = z_2 - z_1$ is

$$\Delta t = \int_{z_1}^{z_2} (dz/v\ (z)) \; .$$

The probability of finding that particle in Δz is $\Delta t/T$ when comparing elements Δz_1 and Δz_2; thus, we have the relative weighting as $\Delta t_2/\Delta t_1$. If the center distribution is known in θ_0, so is the distribution at each point in z where $g_z\ (\theta_0) = g_0(\theta_0)\ \Delta t_2/\Delta t_0\ (g_z \equiv g(z))$.

For the 2XIIB we have $B(z) = B_{min}\ [1 + (z/75)^2]$ (Ref. 2) and conservation of magnetic moment requires

$$B(z_{max}) = B_{min} \frac{|v|^2}{v_{\perp 0}^2} = B_{min} \frac{v_{\parallel 0}^2 + v_{\perp 0}^2}{v_{\perp 0}^2} \quad (z_{max} \equiv \text{turn-around point}),$$

$$1 + \left(\frac{z_{max}}{75}\right)^2 = \cot^2 \theta_0 + 1 \ ,$$

$$z_{max} = 75 \cot \theta_0 \ ,$$

$$T = \int_0^{75 \cot \theta_0} \frac{dz}{|v| \cos \theta} \text{ but } \theta = \theta(z) \ .$$

$$v_\perp{}^2 = B\, v_{\perp 0}^2 / B_{min},$$

$$\frac{\sin^2 \theta}{\sin^2 \theta_0} = 1 + \left(\frac{z}{75}\right)^2 \ ,$$

$$\sin^2 \theta = \left[1 + \left(\frac{z}{75}\right)^2\right] \sin^2 \theta_0 \ ,$$

$$1 - \cos^2 \theta = 1 - \cos^2 \theta_0 + (z/75)^2 \sin^2 \theta_0 \ ,$$

$$\cos^2 \theta = \cos^2 \theta_0 - (z/75)^2 \sin^2 \theta_0 = \cos^2 \theta_0 - \left(\frac{z \sin \theta_0}{75}\right)^2 \ ,$$

and

$$\cos \theta = \sqrt{\cos^2 \theta_0 - \left(\frac{z \sin \theta_0}{75}\right)^2} \ ;$$

therefore

$$T = \int_0^{75 \cot \theta_0} \frac{dz}{|v| \left[\cos^2 \theta_0 - \left(\frac{z \ \ in \ \theta_0}{75}\right)^2\right]^{1/2}} \ .$$

Let $\cos^2 \theta_0 = a^2$, $\dfrac{\sin^2 \theta_0}{(75)^2} = c^2$,

$$|v|T = \int_0^{\sqrt{a/c}} \frac{dz}{(a^2 - c^2z^2)^{1/2}} = \pi/2|v| .$$

$$|v|\Delta t = \int_{z_1}^{z_2} \frac{dz}{v_{\parallel}} = \int_{z_1}^{z_2} \frac{dz}{(a^2 - c^2z^2)^{1/2}}$$

$$= \frac{1}{c} \arcsin \ z\sqrt{c/a} \ ,$$

and

$$\frac{\Delta t}{T} = \frac{\arcsin z_2 \tan \theta_0/75 - \arcsin z_1 \tan \theta_0/75}{\pi/2} \quad .$$

This approach is most applicable when simulating plasma evolution, as we shall discuss later.

The equivalence of this approach to that of Hall and Simonen[1] may be easily recognized. We have[1]

$$n(B,L) = \int_0^{\infty} \varepsilon^{1/2} \, d\varepsilon \int_0^{1/B} d\nu B(1 - \nu B)^{-1/2} \, f(\varepsilon,\nu;L)$$

where

$\varepsilon \equiv$ energy, and $L \equiv$ the longitudinal invariant.

If the distribution is separable in energy and angle then

$$n(B,L) = \int_0^{1/B} d\nu B(1 - \nu B)^{-1/2} \, g(\nu) \ .$$

The total number of particles in the plasma is

$$N = \int_V n(B,L) \, dV$$

$$= \int_0^{\infty} \int_0^{1/B} \int_0^{\infty} \int_0^{2\pi} d\nu B \, (1 - \nu B)^{-1/2} \, g(\nu) \, f(z) \, dz \, f(r) \, r dr d\phi$$

in cylindrical coordinates. (The density of field lines is assumed to have the same dependence as plasma density in r.)

$$N \propto \int_0^{1/B} d\nu B(1 - \nu B)^{-1/2}\, g(\nu) \int_0^{\infty} f(z)dz \ .$$

But $(1 - \nu B)^{-1/2} = v_{\|}\ \sqrt{2\varepsilon}$.

$$\propto \int_0^{1/B} d\nu B \int_0^{\infty} \frac{dz}{v_{\|}}\, f(z)\ g(\nu)$$

or for small Δz (constant $f(z)$) and $B = B_{min}$ (and noting $B_{min}\ d\nu \propto \cos\theta_0$ $d\cos\theta_0 = \cos\theta_0\ d\mu_0$)

$$\frac{dN(z)}{d\nu} \propto B_{min}\ g(\nu)\ \frac{\Delta z}{v_{\|}(z)} \ ,$$

$$\frac{dN}{d\mu_0}\ (z) \propto \cos\theta_0\ g(\nu)\ \frac{\Delta z}{v_{\|}(z)} \ ,$$

$$\propto \frac{dN}{d\mu_0}\ (0)\ \frac{v_{\|}(0)}{v_{\|}(z)} \ ,$$

$$\propto \frac{dN}{d\mu_0}\ \frac{\Delta t_2}{\Delta t_0} \ ,$$

and

$$g_z(\theta_0) \propto g_0(\theta_0)\ \Delta t_2/\Delta t_0 \quad \text{as before.}$$

EXPERIMENTAL APPLICATION

Plasma Evolution

Each channel of the $g(\mu)$ detector includes a readout for dv/dt. This signal is proportional to the instantaneous power entering that channel. A close comparison of signal changes over time will indicate how the plasma evolves in velocity space.

The ANGLE (App. A) has been developed to aid in the investigation of plasma evolution. This code simulates the injection of neutrals into the plasma and their capture at the z-axis, and it subsequently calculates a distribution of all injected particles according to their center angles (θ_0). Since the distribution reflects the center angle of all plasma particles, regardless of position, time averaging provides an estimate of local angular distribution at particular points along the z-axis. Comparison of the code-generated distribution to that calculated by Stallard at $\beta = 0.3$, $z_0 = 0\ \mathrm{cm}^2$ implies that injected distribution is more sharply peaked at higher angles (Fig. 5). This is to be expected. The peculiar "valley" at $\cos\theta_0 = 0$ (Fig. 5) results from the "bending" of the distribution peak in the magnetic well. This valley, of course, will fill up with subsequent particle interaction to reach an equilibrium distribution more coincident to that of Stallard.

Current theory about the 2XIIB plasma evolution primarily centers around four processes. These processes can be ordered by their characteristic times. First, neutrals are injected at nearly constant energy and at nearly perpendicular velocity (Fig. 6a). The time associated with the plasma injection (assuming unity trapping efficiency, cylindrical plasma of 7 cm radius, 40 cm length, and 300 A current) is

$$t_{in} = \frac{\text{number of particles in plasma}}{\text{current}}$$

$$= \frac{[\pi(7\ \mathrm{cm}^2)(40\ \mathrm{cm})](1.2\times10^{14}\ \mathrm{particles/cm}^3)(1.6\times10^{-19}\ \mathrm{C/particles})}{(300\ \mathrm{A})}$$

$$3.94\times10^{-4}\ \mathrm{s}$$

$$= 0.394\ \mathrm{ms}.$$

Next, coulomb scattering causes a general broadening of the distribution (Fig. 6b). The time needed for complete broadening of the distribution is[6]

$$\tau_{\theta_{ii}} = \frac{25.8\sqrt{\pi}\,\varepsilon_0^2 m_i^{1/2}(kT_i)^{3/2}}{q^4 n \ln\Lambda}$$

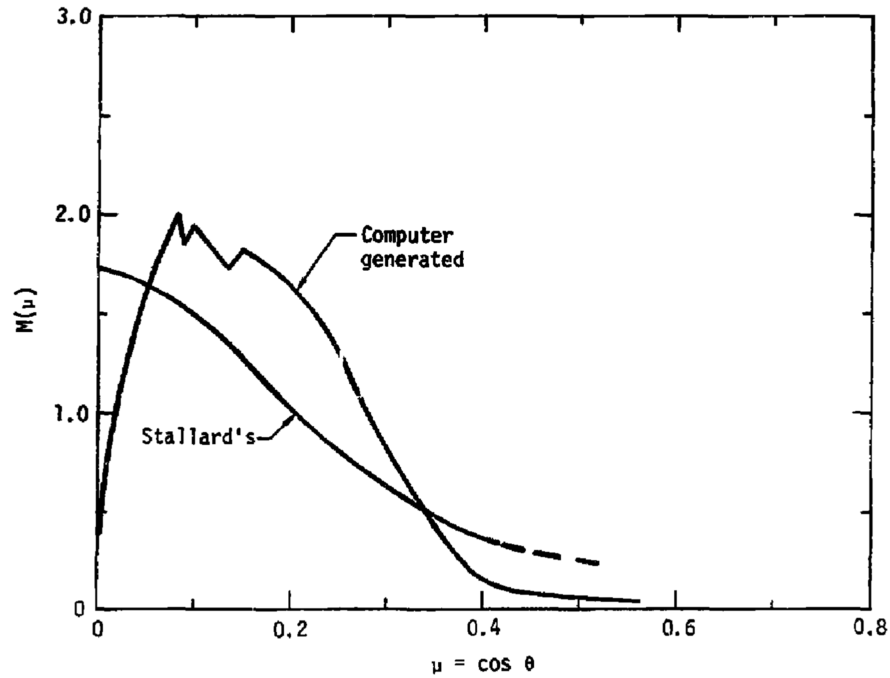

Fig. 5. Stallard and "Angle" M(μ) vs cos θ.

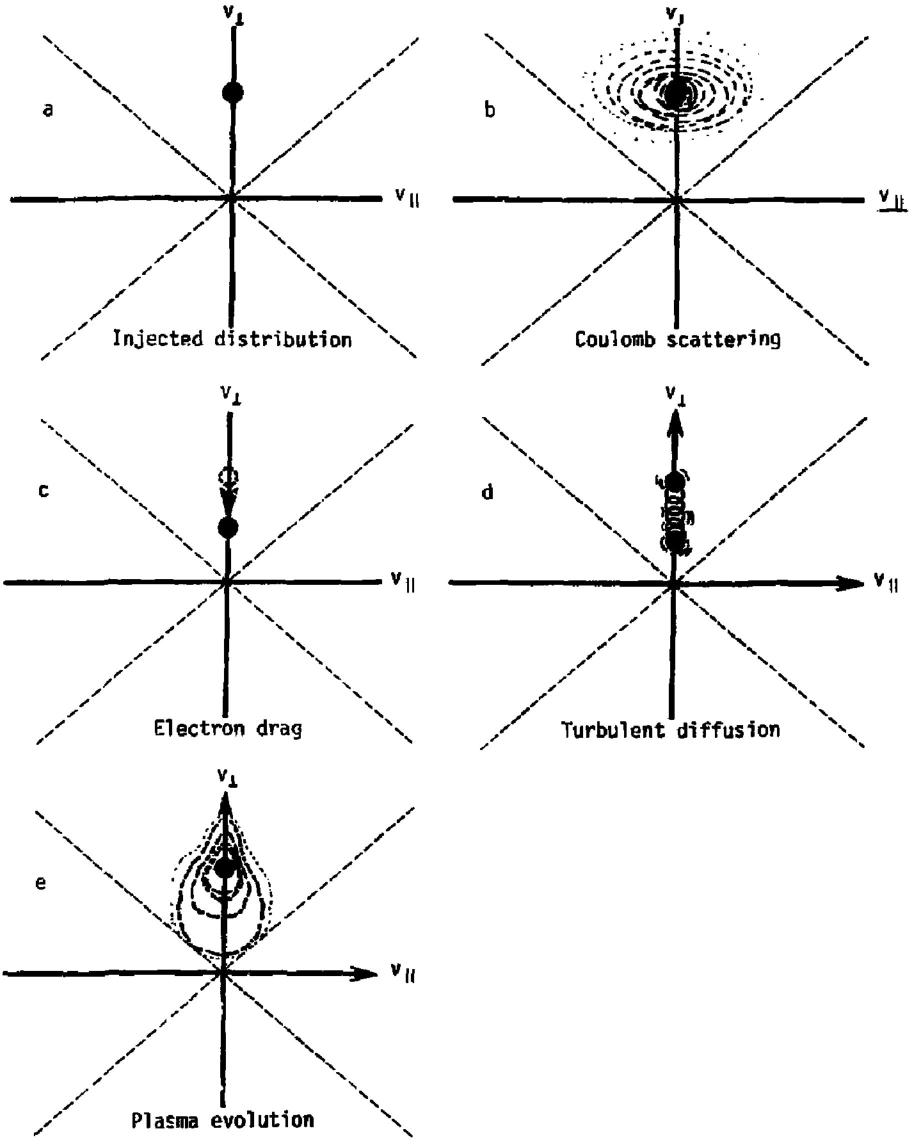

Fig. 6. Velocity-space diagrams.

$$= \frac{25.8\sqrt{\pi}(8.854 \times 10^{-12} f/m)^2 (2 \times 1.67 \times 10^{-27} kg)^{1/2} (1.6 \times 10^{-19} J/eV) T_i^{3/2}\ (eV)}{(1.6 \times 10^{-19}\ C)^4 n \ln \Lambda}$$

where

$$\Lambda = \frac{12\pi(\epsilon_0 kT_e/e^2)^{3/2}}{n_e^{1/2}} .$$

For T_e = 100 eV and $n_e = n = 10^{20}\ m^{-3}$ we have $\ln \Lambda \approx 14.25$ so that

$$\tau_{\theta_{ii}} = 1.42 \times 10^{12} T_i^{3/2}\ (eV)/n$$

$$= 10.1\ ms$$

for T_i = 9 keV.

Electron drag may also contribute to plasma evolution by slowing down the ions as heat is passed to the electrons (Fig. 6c). For electron drag we have[6]

$$n_i \frac{dE_i}{dt} = \frac{q_e^2 q_i^2 n_e n_i m_e \ln \Lambda \left[1 - (2E_i/3kT_e)\right]}{2\pi\varepsilon_0^2 (2\pi m_e kT_e)^{1/2} m_i \left[1 + (4/3\sqrt{\pi})\left(\frac{m_e E_i}{m_i kT_e}\right)^{3/2}\right]}$$

or

$$\tau_{ed} = \frac{E_i 2\pi\varepsilon_0^2 (2\pi m_e kT_e)^{1/2} m_i \left[1 + (4/3\sqrt{\pi})(m_e E_i/m_i kT_e)^{3/2}\right]}{q_e^2 q_i^2 n_e m_e \ln \Lambda \ [1 - 2E_i/3kT_e]}$$

$$\approx \frac{2\pi(8.854 \times 10^{-12} f/m)^2 [2\pi(0.91 \times 10^{-30} kg)]^{1/2} (2 \times 1836) \left[1 + \frac{4}{3}\sqrt{\pi} \left(\frac{T_i}{2 \times 1836\ T_e}\right)^{3/2}\right] T_i}{(1.6 \times 10^{-19}\ C) \ln \Lambda \left[1 - \frac{2T_i}{3T_e}\right] n}$$

$$\approx \frac{4.44 \times 10^{13} T_e^{3/2} (eV)}{n} \quad \text{for } T_i \gg T_e .$$

$$\tau_{ed} \approx 0.44\ ms$$

where

$$\tau_{ed} \equiv [-E_i/(dE_i/dt)] \ .$$

The final process is turbulent diffusion of ions as a result of ion-cyclotron fluctuation. From previous data,[2] $\Delta E/\Delta t$ = 112 eV/μs or $\tau = E_i/(\Delta E/\Delta t)$ = 0.080 ms (E_i ≈ 9 keV). This diffusion tends to increase or decrease perpendicular ion velocity (Fig. 6d).

The superposition of these different processes projects a "tear-drop" evolution in velocity space (Fig. 6e). The dv/dt capability of the g(μ) detector allows a direct plot of plasma angular distribution in velocity space. Spread in $|\bar{v}|$ can be determined from the multichannel 90° cx analyzer so that a complete "moving picture" of the plasma evolution in velocity space is possible.

Axial density measurements may be used to obtain angular distribution; however, obtaining this time evolution would require a series of rather laborious calculations for each time frame considered as opposed to the continuous readout of the dv/dt portion of the g(μ) detector. Until the plasma has attained a stable density distribution, one cannot be sure whether the axial density has reached equilibrium for a particular angular distribution or whether axial-density variations only reflect local transient behavior.

Plasma Shape

The shape (and thus the volume) of the plasma is of continuing interest. It has generally been conceded that the plasma is confined to flux tubes defined by field lines. Stallard's calculation of density utilized this assumption in that

$$\langle n_z \rangle = \frac{\int n dl}{l_z}$$

where l_z is the flux-tube thickness at position z. Larry Hall and others, however, have surmised that the plasma may be confined to p(B) surfaces.

As a check on plasma shape, the $\int n dl$ was calculated with the p(B) surface assumption. A radial density of $n = n_0 e^{-(r/7.35)^2}$ (Ref. 2) was assumed; densities were then calculated at contours of constant $|B|$ (Fig. 7). The constant $|B|$ mapping was obtained from Anderson's 2XIIB[6] code for β = 0.3.

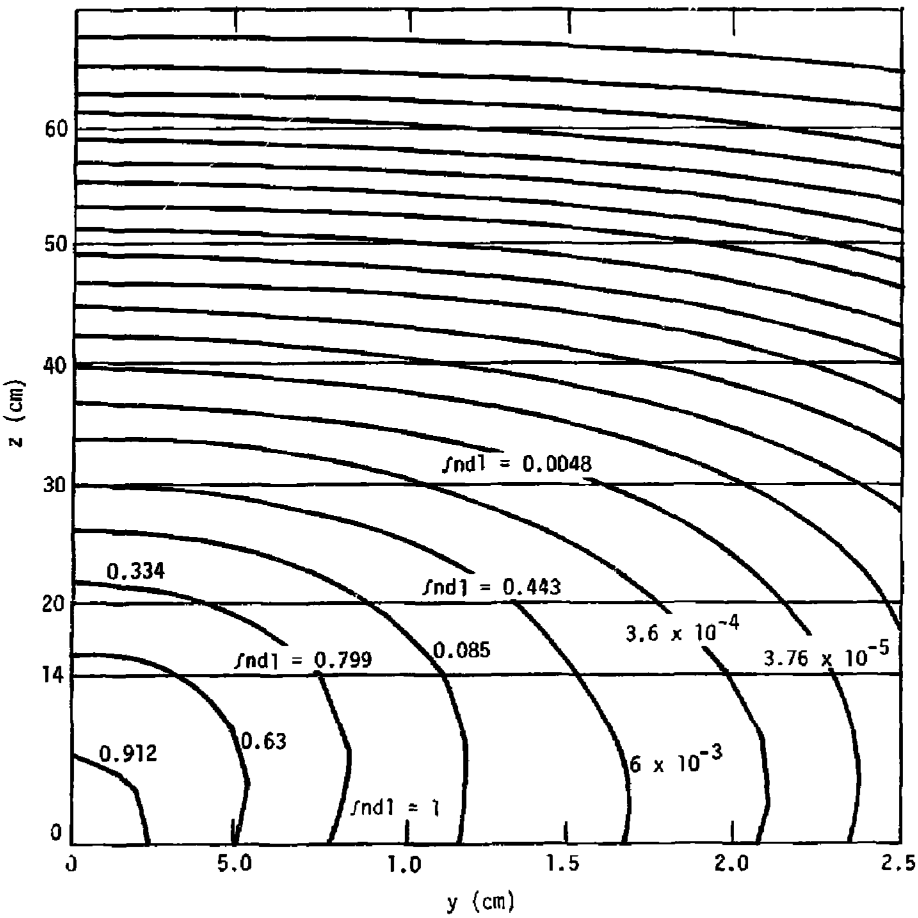

Fig. 7. |B| contours.

The $\int ndl$ at various positions was approximated using a trapezoidal sum rule. Results of these calculations and Stallard's measured data are clearly in conflict (Fig. 8). In fact, for p(B) the $\int ndl$ variation in z is more approximately Gaussian (Fig. 9) than the measured exponential fit.

Taking the measured values of $\int ndl$ to be exponential and assuming separability of n(r,z) into n(0,0)f(r)g(z), the variation in z must also be exponential. We have

$$
\begin{aligned}
ndl &= \int n(r,z)dl \\
&= n(0,0) \int f(r)g(z)dr \\
&= n(0,z) \int e^{-(r/7.35)^2}\, dr \\
&\propto n(0,z)
\end{aligned}
$$

so that n(0,z) varies as $\int ndl$.

If we instead assume separability of n(r,z) into $n(r,z) = n(0,z)\, e^{-[r/7.35f(z)]^2}$, where f(z) is a factor which takes into account the change in line length because of compression or expansion, we have

$$
\begin{aligned}
\int_0^r n(r,z)dl &= \int_0^r n(0,z)e^{-[r/7.35f(z)]^2}\, dr \\
&= n(0,z) \int_0^r e^{-[r/7.35f(z)]^2}\, dr \\
&= n(0,z)\, E_1\, [r/7.35f(z)]^2 \Big|_0^r
\end{aligned}
$$

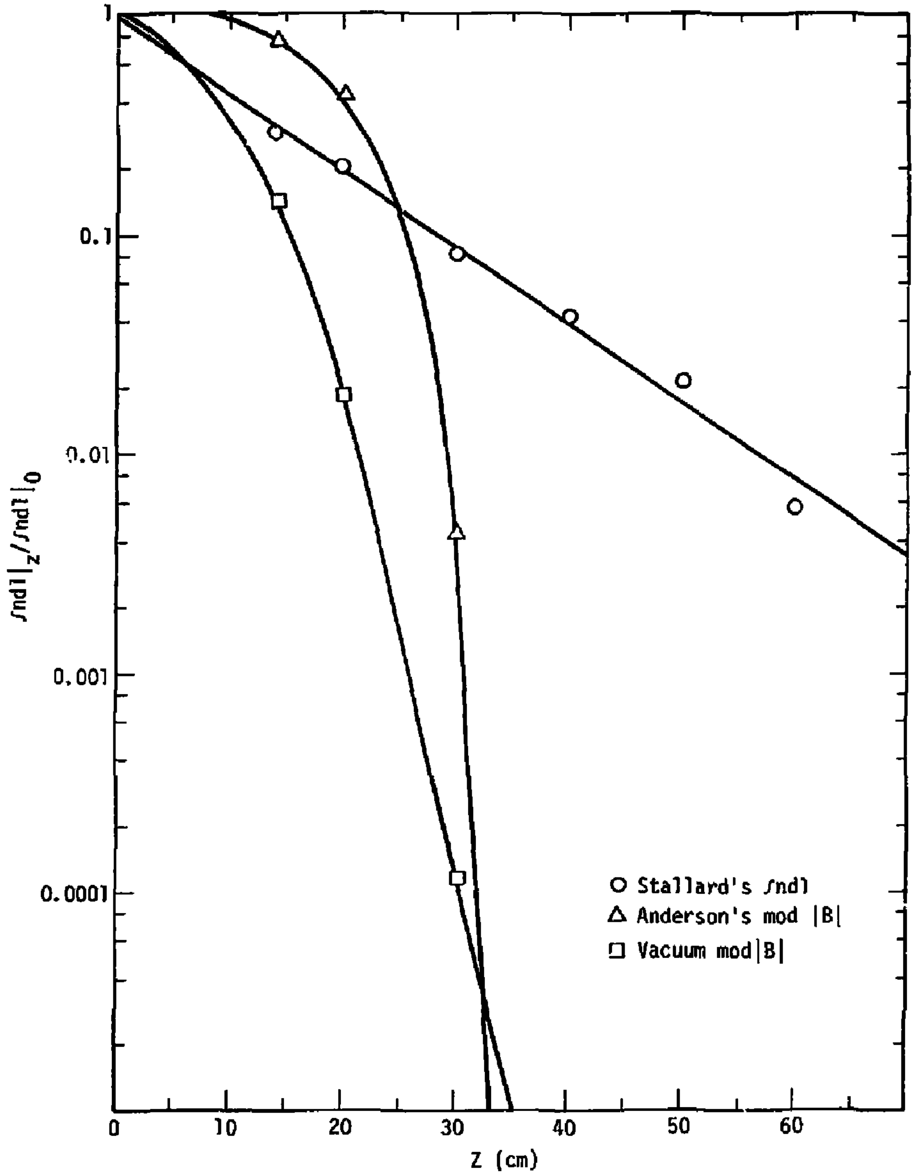

Fig. 8. Stallard and p(B) vs z.

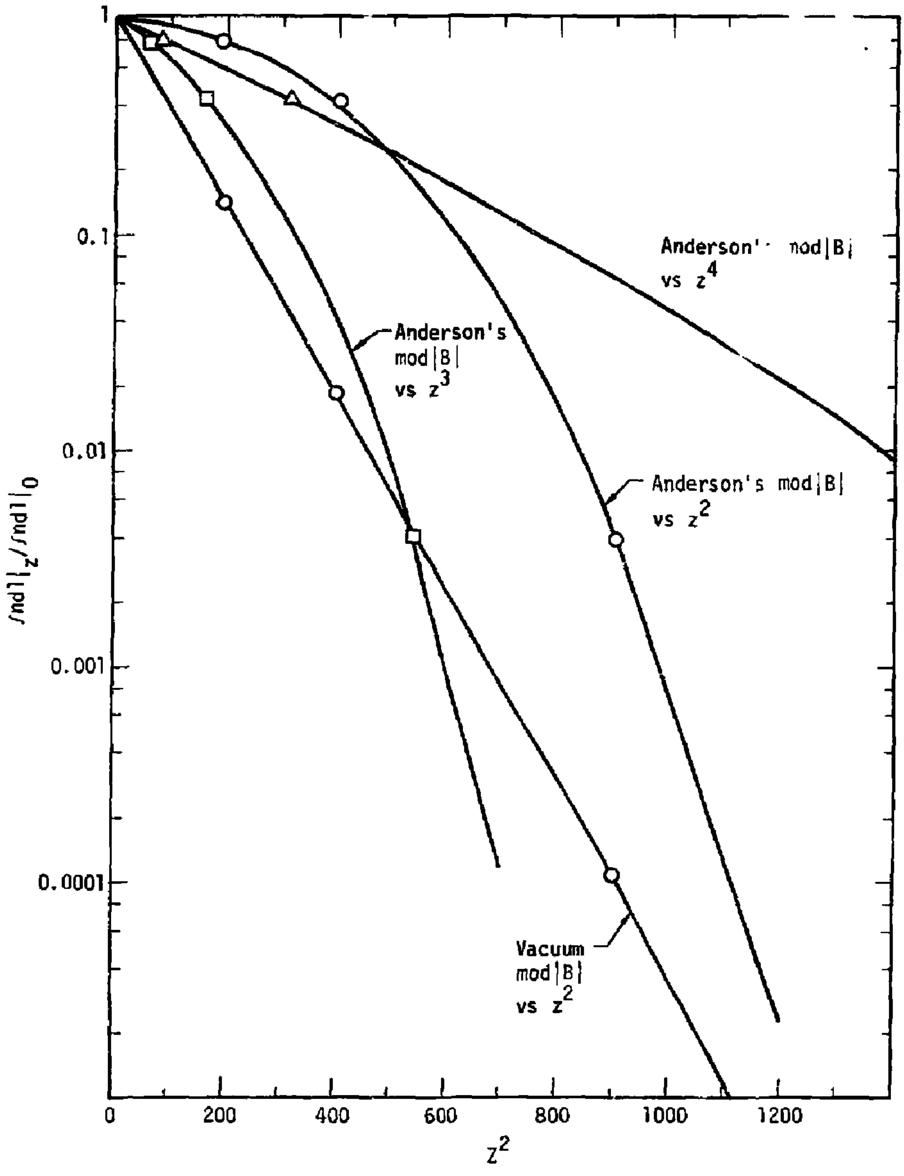

Fig. 9. p(B) vs z^2 (z^3 and z^4).

or in the limit $r \to \infty = n(0,z)\ f(z)\ 7.35\ \sqrt{\pi/2}$ so that $n(z) \propto \int n dl/f(z)$. However, the graph of f(z) in the region where $\int dnl$ has been measured shows that f(z) is also an exponential (Fig. 10) so that n(z) must again be described as an exponential. Taking the flux-tube assumption as correct, we have the best fit for $n(z) = 0.95\ n(0)\ e^{-[z/20.1]}$ (Fig. 11).

Another check on plasma shape may be obtained from a measure of angular distribution. As outlined in Ref. 1, the density profile in z may be directly obtained from angular distribution. Stallard has calculated the angular distribution that should exist for a flux-tube shape. For comparison we can calculate the distribution expected from a p(B) surface.

For the density variation in r, let us take $n(r) = n_0\ e^{-[r/7.35]^2}$. Then for the vacuum B field we have

$$B_0 = B_{0min}\left[1 + \left(\frac{r}{55}\right)^2\right]\ (B_0 \equiv B_{vac})$$

and correcting for β

$$\frac{B(r)^2}{8\pi} = \frac{B_0(r)^2}{8\pi} - n(r)\ kT$$

in the plane $z = 0$. Since contours of constant $|B|$ define contours of constant n, we have

$$B(r) = \sqrt{B_0(r)^2 - \beta B^2_{0\ min}\ e^{-(r/7.35)^2}} \text{ where } \beta = \frac{n_0 kT}{B^2_{0\ min}/8\pi}$$

$$= B_{0\ min}\sqrt{\left[1 + (r/55)^2\right]^2 - \beta e^{-(r/7.35)^2}}\ ,$$

and

$$\frac{B(r)^2}{B_0^2\ (0)} = 1 + 2(r/55)^2 + (r/55)^4 - \beta e^{-(r/7.35)^2}\ .$$

Let us approximate $(r/55)^2 << 1$ so that

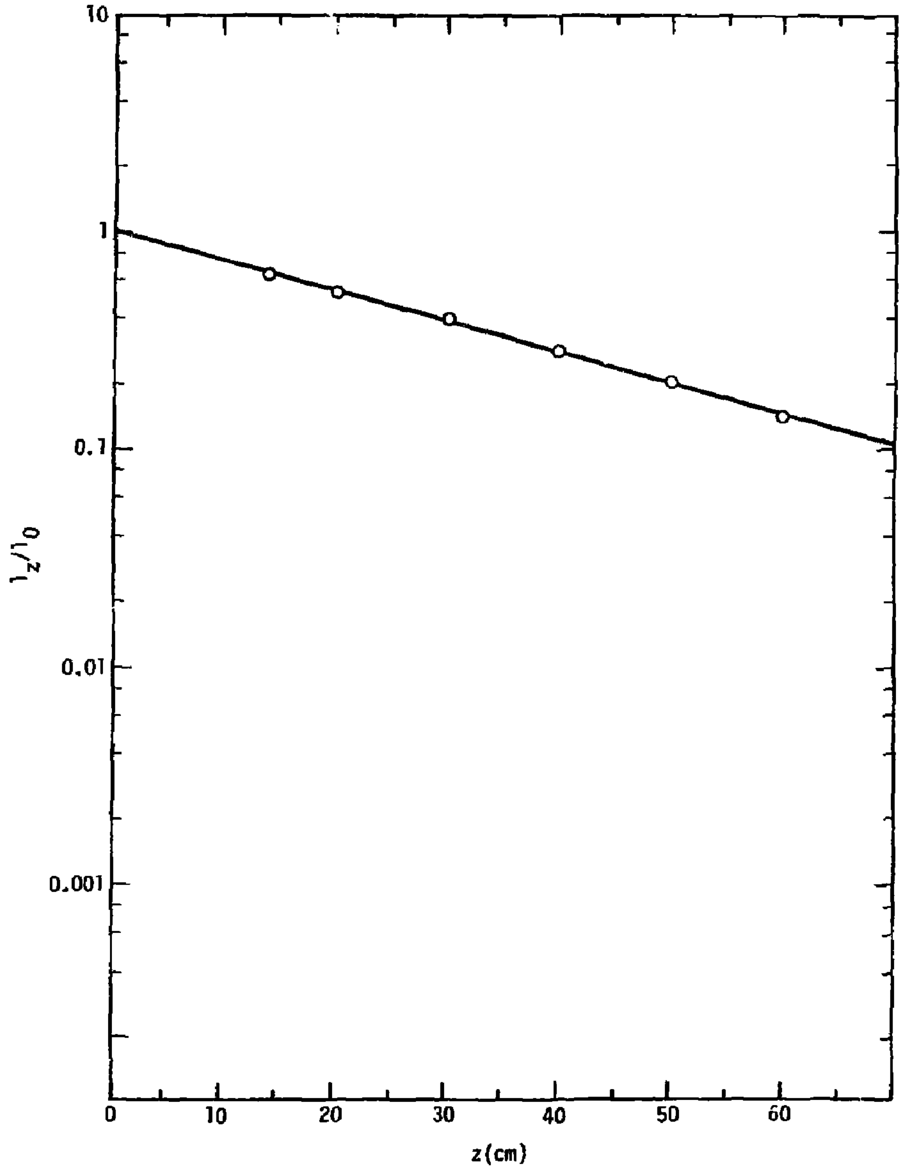

Fig. 10. I(z)/I(ϕ) vs z.

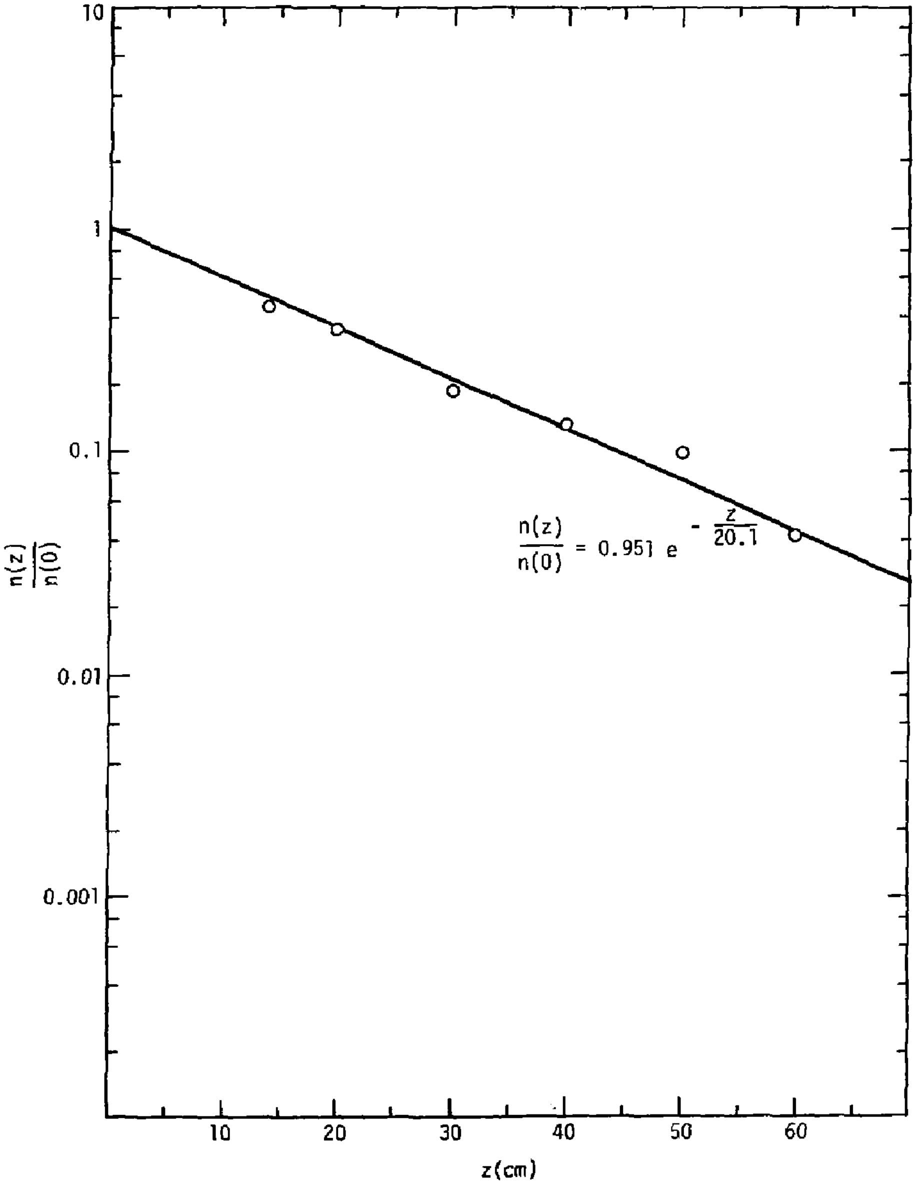

Fig. 11. n(z)/n(ϕ) vs z.

$$e^{-(r/7.35)^2} = \frac{1}{\beta}\left[1 - \frac{B^2(r)}{B_0^2\ (0)}\right] ;$$

for

$$n = n(0)e^{-(r/7.35)^2}$$

$$n(B)/n(B_{min}) = \frac{1}{\beta}\left[1 - \frac{B^2(r)}{B_0^2\ (0)}\right] ,$$

and

$$\frac{n(\rho)}{n(B_{min})} = \frac{1}{\beta}\left[\frac{\rho^2\ B_0^2\ (0) - 1}{\rho^2\ B_0^2\ (0)}\right] \quad \left(\rho \equiv \frac{1}{B}\right).$$

For our limits on ρ we have

$$\frac{1}{\beta}\left[\frac{\rho^2\ B_0^2\ (0) - 1}{\rho^2\ B_0^2\ (0)}\right] = 1 ,$$

$$\rho^2\ B_0^2\ (0) - 1 = \beta\ \rho^2\ B_0^2\ (0) ,$$

$$\rho^2 = \frac{1}{0.7\ B_0^2\ (0)} ,$$

$$\rho_{max} = \left(\frac{1}{1 - \beta}\right)^{1/2} \frac{1}{B_0\ (0)} ,$$

$$\rho_{min} = \frac{1}{B_0\ (0)} ,$$

$$\therefore\ n(\rho) = \frac{n(B_{min})}{\beta}\left[\frac{\rho^2\ B_0^2\ (0) - 1}{\rho^2\ B_{0\ min}^2(0)}\right] \rho_{min} \le \rho \le \rho_{max}$$

$$= 0 \quad \rho > \rho_{max}\ \rho > \rho_{min}.$$

From the Hall-Simonen paper[1] we have

$$Q(\nu) = \frac{d}{d\nu}\left(\pi^{-1}\int_0^{\nu} (\nu - p)^{-1/2}\rho^{1/2} n(\rho)\, d\rho\right),$$

$$= \frac{d}{d\nu}\left(\pi^{-1}\int_{\rho_{min}}^{\nu} \frac{1 - 1/\left(\rho^2 B_0^2\right)_{min}}{\sqrt{\nu\,\rho}}\,\rho^{1/2}\, d\rho\right)\frac{n(B_{min})}{\beta}$$

$$= \frac{d}{d\nu}\left(\int_{\sqrt{\rho_{min}}}^{\sqrt{\nu}}\left[\frac{x^2}{\sqrt{\nu - x^2}} - \frac{1}{x^2\sqrt{\nu - x^2 B_{0\ min}^2}}\right]dx\right)\frac{2n(B_{min})}{T\beta}\quad (x^2 \equiv \rho)$$

$$= \frac{d}{d\nu}\left[-\frac{x}{2}\sqrt{\nu - x^2} + \frac{\nu}{2}\sin^{-1}\frac{x}{\sqrt{\nu}} + \frac{\sqrt{\nu - x^2}}{\nu x B_{0\ min}^2}\right]\int_{\sqrt{\rho_{min}}}^{\sqrt{\nu}}(dx)$$

$$= \frac{d}{d\nu}\left[\frac{\nu\pi}{4} + \frac{\sqrt{\rho_{min}}}{2}\sqrt{\nu - \rho_{min}} - \frac{\nu}{2}\sin^{-1}\frac{\sqrt{\rho_{min}}}{\nu} - \frac{\sqrt{\nu - \rho_{min}}}{\nu\sqrt{\rho_{min}}\, B_{0\ min}^2}\right](dx)$$

$$= \frac{\pi}{4} + \frac{\sqrt{\rho_{min}}}{2}\,\frac{1}{2\sqrt{\nu - \rho_{min}}} - \frac{1}{2}\sin^{-1}\frac{\sqrt{\rho_{min}}}{\nu} + \frac{\nu}{2}\,\frac{1}{\sqrt{\nu - \rho_{min}/\nu}}$$

$$+ \frac{1}{2}\,\frac{\sqrt{\rho_{min}}}{\nu}\,\frac{1}{\nu} + \frac{\sqrt{\nu\,\rho_{min}}}{\nu^2\sqrt{\rho_{min}}\, B_{0\ min}^2} - \frac{1}{2}\,\frac{1}{\nu\sqrt{\rho_{min}}\, B_{0\ min}^2\sqrt{\nu - \rho_{min}}}$$

$$= \frac{\pi}{4} + \frac{\sqrt{\rho_{min}}}{2} \frac{1}{\sqrt{\nu - \rho_{min}}} - \frac{1}{2} \sin^{-1} \frac{\sqrt{\rho_{min}}}{\nu}$$

$$+ \frac{\sqrt{\nu - \rho_{min}}}{\nu^2 \sqrt{\rho_{min}}\, B^2_{0\ min}} - \frac{\rho_{min} \sqrt{\rho_{min}}}{2\nu \sqrt{\nu - \rho_{min}}} \ .$$

Solving for r at $B = B_0(0) = B_{max}$ we have

$$\beta_e^{-(r/7.35)^2} \approx 2(r/55)^2 \quad \text{or } r_{max} \approx 10 \text{ cm}$$

so that $2(r_{max}/55)^2 \approx 0.05$ and our approximation $(r/55)^2 << 1$ is fairly accurate.

The characters of this distribution and the flux-tube distribution are markedly different (Fig. 12); for the flux-tube assumption we would expect to measure nearly all charge-exchange signals in the first channel. However, for the $p(B)$ assumption we would expect signals in the first two channels to be nearly equal, while no signal would be expected for the other channels. Clearly the $g(\mu)$ detector should indicate which shape most accurately describes the 2XIIB plasma.

Broadening of Angular Distribution

The final use of the $g(\mu)$ detector is perhaps the most direct and the most important. Current theory of plasma pressure requires that $p_\perp$ and $p_\parallel$ meet specific relational constraints for stability. Specifically we would expect the detector to measure a broader distribution (greater $p_\parallel/p_\perp$) if current theory holds.

In addition, this experiment will directly indicate the depth of the magnetic well "dug" by the plasma as reflected in a broadening of angular distribution. ANGLE (App. A) was developed to measure injected distribution but it has also been used to measure the β effect on angular distribution. Some indication of the expected broadening is given in a graph of average

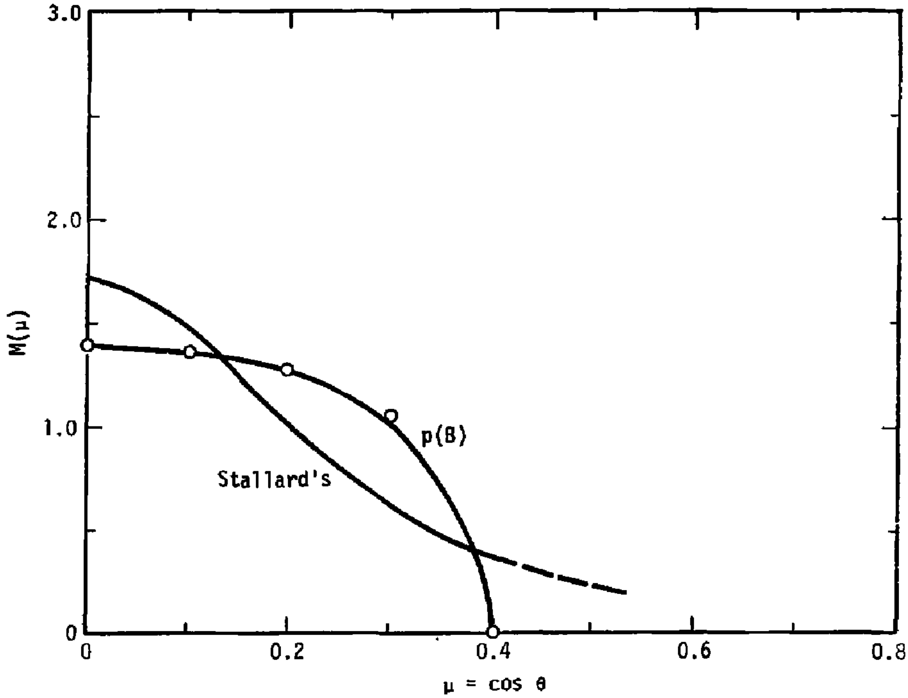

Fig. 12. p(B) and flux M(μ) vs cos θ.

center angle vs β (Fig. 13). While the approximations used to measure this relationship do not hold well for very high β, the effect of high β on the lowering of the average center angle should certainly be well defined.

CONCLUSIONS

The $g(\mu)$ detector provides a direct measure of the angular distribution of 2XIIB plasma. Applications of the $g(\mu)$ detector are allied to the characteristics of the 2XIIB but may be extended to other machines by proper choice of shape and material. Signal strength estimates at the detector indicate a 2% isotropic distribution strength should be detectable giving a "fine" indication of distributional shape.

We can utilize time-averaging techniques to estimate injected angular distribution. Monte-Carlo simulation of injection shows the injected distribution is more sharply peaked than the equilibrium distribution calculated by Stallard. In addition, the injected distribution at 90° is not a maximum. The $g(\mu)$ detector provides a direct measurement of plasma evolution from injected to equilibrium distribution.

Plasma is currently assumed to follow a flux tube rather than a $p(B)$ surface. If density were separable in r and z, microwave measurements would show that the plasma must be flux-tube shaped. Using the Hall-Simonen[1] paper, however, we can verify by the $g(\mu)$ detector which shape is most accurate. Regardless of plasma shape, the density variation in z is exponential and not Gaussian as previously assumed.

ACKNOWLEDGMENTS

Credit must go to Grant Logan for the original design and concept of the $g(\mu)$ detector. I also wish to thank Barry Stallard for the use of his microwave data and assistance in its interpretation, Larry Hall for discussion of the plasma shape and its various implications, Tom Simonen and Grant Logan for their invaluable guidance, and Judy Bailey and Mary Lou Nelson for their patient help in the preparation of this report.

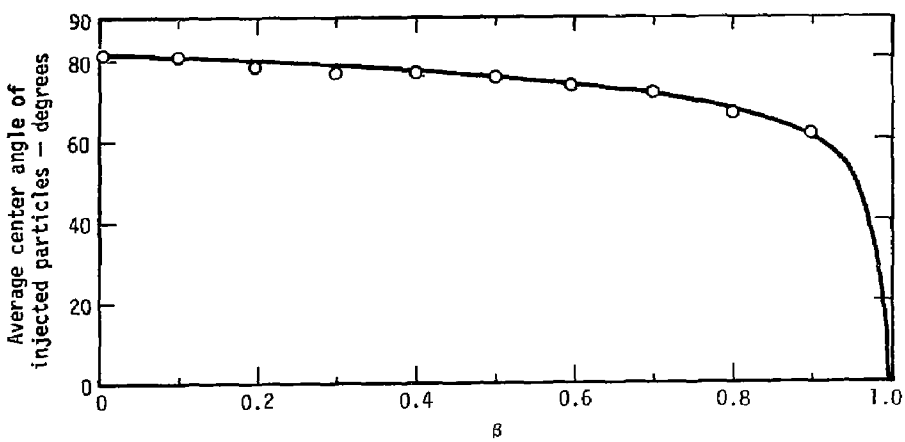

Fig. 13. Average angle at center vs β.

REFERENCES

1. L. S. Hall and T. C. Simonen, *Phys. Fluids* 17, 1014 (1974).
2. F. H. Coensgen, J. F. Clauser, D. L. Correll, W. F. Cummins, C. Gormezano, B. G. Logan, A. W. Molvik, W. E. Nexsen, T. C. Simonen, B. W. Stallard, and W. C. Turner, *Status of 2XIIB Plasma Confinement Experiments*, Lawrence Livermore Laboratory, Rept. UCID-17037 (1976).
3. K. H. Berkner, W. R. Baker, W. S. Cooper, K. W. Ehlers, W. B. Kunkel, R. V. Pyle, and J. W. Stearns, "Performance of LBL 20 kV, 10-A and 50-A Neutral-Beam Injectors," in *Proc. Symp. 4th Int. Conf. Plasma Phys. and Cont. Fusion Res., Tokyo 1974*, (vol. 1, IAEA, Vienna 1975, p. 329).
4. C. Gormezano, *Beam Trapping by the Plasma and Energy Lifetime*, Lawrence Livermore Laboratory, internal Memo (1976).
5. R. L. Freeman and E. M. Jones, *Atomic Collision Processes in Plasma Physics Experiments*, Culham Laboratory Rept. CLM-R137 (1974).
6. D. V. Anderson and J. Breazeal, *VPEC: A 3D Vector Potential Equilibrium Code for High Beta Minimum-B Plasma Confinement*, Lawrence Livermore Laboratory (to be published as UCRL).

JC/lc/mg/mla/jf

APPENDIX A
ANGLE

We must calculate injected-ion angular distribution to properly interpret the later evolution of equilibrium angular distribution. The ion source, however, is geometrically complicated.

The 12 ion sources each consist of a uniform series of beamlets arranged along a 35-cm strip parallel to the z-axis. Each beamlet is aimed at a common point, but neutrals are injected with a Gaussian spatial distribution in both "up-down" and "side-to-side" directions. If we define the horizontal plane as a plane containing the source and the z axis and the vertical plane as a plane perpendicular to both the z-axis and the source line, then we may define θ_y as the angle between the neutral trajectory and the source center-target line projected on the vertical plane. Likewise θ_z is the angle (defined by the projections) on the horizontal plane. The beam may then be described by the equation

$$S = S_0\, e^{-(\theta_0/2°)^2}\, e^{-(\theta_y/0.6°)^2} .$$

We can then calculate $\langle\mu\rangle = \langle\cos\theta\rangle$ as a measure of angular spread if we first assume that all ions are trapped on the z-axis ($\theta_y = 0$) with unit-trapping efficiency. Then

$$\langle\mu\rangle = \iint S dl\, d\theta_z \cos\theta \Big/ \iint S dl\, d\theta_z$$

$$= \iint S dl\, d\theta_z \sin\theta_i \Big/ \iint S dl\, d\theta_z$$

$$= \iint S_0\, e^{-(\theta_z/2°)^2} \sin(\theta_z + \theta_t)\, dl d\theta_z \Big/ \iint S_0\, e^{-(\theta_z/2°)^2}\, dl d\theta_z .$$

By the geometry of Fig. A1 we have $-\theta_z = \arcsin(1 - t/r)$ and small $\theta_t \approx (t - 1/r)$. For small $\theta_z + \theta_t = \theta_i$,

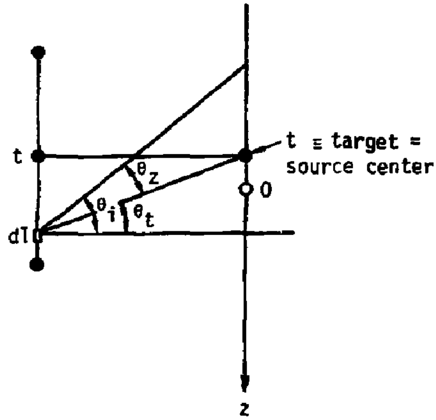

Fig. A1. Source-target geometry.

$$\theta_i = \theta_z + \theta_t$$

$$\frac{z - l}{r} = \theta_z + \theta_t$$

and

$$\theta_z \approx \frac{z - t}{r} .$$

Finally, we can change from θ_z to z

$$\langle\mu\rangle \approx \int_{-\infty}^{\infty}\int e^{-(z-t/2°r)^2} \left|\left(\frac{z - l}{r}\right)\right| \, dl \, dz \Big/ \int_{-\infty}^{\infty}\int e^{-(z-t/2°r)^2} \, dl \, dz$$

$$= \int_0^{\infty}\int e^{-(z-t/2°r)^2} \left(\frac{z - l}{r}\right) dl \, dz \Big| \int_0^{\infty}\int e^{-(z-t/2°r)} \, dl \, dz .$$

The sources are arranged in a symmetric pattern (Fig. 3) at radii of r_1 = 330 cm, r_2 = 380 cm so that small θ_i and $\theta_{z_1} = \theta_{z_2} \approx 2°$, z_1 = 11.5, and z_2 = 13.3. If t = 0 we then have for r = 330 cm[1]

$$\langle\mu\rangle = \frac{\int_1^{\infty}\int_{-17.5}^{17.5} e^{-(z/11.5)^2} (z - l/330) \, dl \, dz}{\int_1^{\infty}\int_{-17.5}^{17.5} e^{-(z/11.5)^2} \, dl \, dz}$$

but

$$\int_1^{\infty}\int_{-17.5}^{17.5} = \int_{17.5}^{\infty}\int_{17.5}^{17.5} + \int_{-17.5}^{17.5}\int_{-17.5}^{z} .$$

Therefore

$$\langle\mu\rangle = \frac{\left\{\frac{1}{330}\int_{17.5}^{\infty} e^{-\left(\frac{z}{11.5}\right)^2}\left(z1 - \frac{1^2}{2}\right)\Bigg|_{-17.5}^{17.5} dz + \int_{-17.5}^{17.5} e^{-\left(\frac{z}{11.5}\right)^2}\left(z1 - \frac{1^2}{2}\right)\Bigg|_{-17.5}^{z} dz\right\}}{\left[35\int_{17.5}^{\infty} e^{-\left(\frac{z}{11.5}\right)^2} dz + \int_{-17.5}^{17.5} e^{-\left(\frac{z}{11.5}\right)^2} 1\Bigg|_{-17.5}^{z} dz\right]}$$

$$= \frac{\frac{1}{330}\int_{17.5}^{\infty} e^{-\left(\frac{z}{11.5}\right)^2} 35\ z\ dz + \int_{-17.5}^{17.5} e^{-\left(\frac{z}{11.5}\right)^2}\left(\frac{z^2}{2} + 17.5z + \frac{17.5^2}{2}\right) dz}{35\int_{17.5}^{\infty} e^{-\left(\frac{z}{11.5}\right)^2} dz + \int_{-17.5}^{17.5} e^{-\left(\frac{z}{11.5}\right)^2}(z + 17.5)\ dz}$$

$$= \frac{\frac{1}{330}\left\{35\left(\frac{11.5}{2}\right)^2 e^{-\left(\frac{17.5}{11.5}\right)^2} - (11.5)^3\left[2\left(\frac{17.5}{11.5}\right) e^{-\left(\frac{17.5}{11.5}\right)^2} - \frac{\sqrt{2\pi}}{\sqrt{2}}(0.9684)\right] + (11.5)\left(\frac{17.5^2}{2}\right)(0.9684)\frac{\sqrt{2\pi}}{\sqrt{2}}\right\}}{(11.5)\left[35\frac{\sqrt{2\pi}}{\sqrt{2}}(0.0158) + 17.5\frac{\sqrt{2\pi}}{\sqrt{2}}(0.9684)\right]}$$

$$= \frac{\frac{1}{330}(228.4 + 2153.6 + 3022.6)}{[17.5\sqrt{\pi}\,(11.5)]}$$

$$= 0.046$$

$$\langle\vartheta\rangle \equiv \arccos\langle\mu\rangle = 87.4°.$$

We now include the effect of mirroring and finite β to obtain the average center angle of injected particles. For our experiment we have $B(Z)/B_{min} = 1 + (Z/75)^2$ (Ref. 2) To conserve magnetic moment we must first require that

$$\theta_0 \equiv \theta_{center} = \arcsin\sqrt{\frac{B_{min}}{B_i}}\cos\theta_i \quad (B_i \equiv \text{injected position B}).$$

For a long-thin approximation of finite β we have:

$$p + B^2/8\pi = \text{const},$$

$$nkT + B^2/8\pi = B^2_{min}/8\pi \ ,$$

and

$$n(Z)kT + B(Z)^2/8\pi = B^2_{min}(Z)/8\pi \ .$$

For $\beta = 0.3$ we have

$$\frac{B(Z)^2}{8\pi} = B_0^2(Z)/8\pi - \beta\ n(Z)/n(0)\ B_0(0)^2/8\pi \ ,$$

$$B(Z)^2 = B_0^2(Z) - \beta\ e^{-Z/17}\ B_0(0)^2$$

and

$$B(Z)^2/B_0(0)^2 = [1 + (z/75)^2] - \beta\ e^{-z/17} \ .$$

We calculate $\langle\mu_0\rangle = \langle\cos\ \theta_0\rangle$

$$\sin\ \theta_0 = \sqrt{B_{min}/B_i}\ \cos\ \theta_i \ ,$$

$$\sin^2\ \theta_0 = B_{min}/B_i\ \cos^2\ \theta_i \ ,$$

and

$$1 - \cos^2\ \theta_0 =$$

$$\cos^2\ \theta_0 = \left(1 - B_{min}/B_i\ \cos^2\ \theta_i\right)^{1/2}$$

$$= 1 - \left[\frac{\cos^2\ \theta_i\ \sqrt{1 - \beta}}{\{[1 + (z/75)^2] - \beta\ e^{-z/17}\}^{1/2}}\right]^{1/2} \ .$$

We may now write

$$\langle\mu\rangle = \langle\cos\theta_0\rangle = \frac{\displaystyle\int_0^\infty \int_{-17.50}^{17.50} e^{-\left(\frac{z}{11.5}\right)^2} \cos\theta_0 \, dz \, dl}{\displaystyle\int_0^\infty \int_{-17.50}^{17.50} e^{-\left(\frac{z}{11.5}\right)^2} \, dz \, dl}$$

$$\approx \frac{\displaystyle\int_0^\infty \int_{-17.5}^{17.5} e^{-\left(\frac{z}{11.5}\right)^2} \; 1 - \left\{\frac{\left[1 - \left(\frac{z - l}{330}\right)^2\right]\sqrt{1-\beta}}{\left[1 + \left(\frac{z}{75}\right)^2 - \beta\, e^{-\left(\frac{z}{17}\right)}\right]^{1/2}}\right\}^{1/2} dz}{[(35)(11.5)\sqrt{\pi/2}]} \;.$$

If we let $f = 1 + (z/75)^2 - \beta\, e^{-z/17}$, we have

$$\left\{1 - \frac{\left[1 - \left(\frac{z - l}{300}\right)^2\right]\sqrt{1-\beta}}{\left[1 + \left(\frac{z}{75}\right)^2 - \beta\, e^{-\left(\frac{z}{17}\right)}\right]^{1/2}}\right\}^{1/2} = \left\{1 - \frac{\left[1 - \left(\frac{z - l}{300}\right)^2\right]\sqrt{1-\beta}}{f^{1/2}}\right\}^{1/2}$$

$$= \left(\frac{1-\beta}{f}\right)^{1/4} \left\{\left(\frac{f}{1-\beta}\right)^{1/2} - 1 + \left(\frac{z - l}{300}\right)^2\right\}^{1/2}$$

$$= \left(\frac{1-\beta}{f}\right)^{1/4} \frac{1}{300} \left\{\left(\sqrt{\frac{f}{1-\beta}} - 1\right) 300^2 + (z - l)^2\right\}^{1/2}$$

$$= \left(\frac{1-\beta}{f}\right)^{1/4} \frac{1}{300} \left\{330^2 \left(\sqrt{\frac{f}{1-\beta}} - 1\right) + z^2 - 2z\,l + l^2\right\}^{1/2}$$

$$= \frac{1}{330} \left(\frac{1-\beta}{f}\right)^{1/4} \sqrt{g - 2z\,l + l^2}$$

where

$$g = 330^2 \left(\sqrt{\frac{f}{1-\beta}} - 1\right) + z^2 \;.$$

From the tables we find that

$$\int_{-17.5}^{17.5} \sqrt{g - 2zl + l^2}\, dl = \frac{1}{2} \left\{ (l - z)\sqrt{l^2 - 2zl + g} \right.$$

$$\left. + (g - z^2) \left[\log\left(\sqrt{l^2 - 2zl + g} + (l - z)\right) \right] \right\} \int_{-17.5}^{17.5}$$

$$= \frac{1}{2} \left\{ (17.5 - z) \sqrt{(17.5)^2 - 35z + g} + (17.5 + z) \sqrt{(-17.5)^2 + 35z + g} \right.$$

$$+ (g - z^2) \left[\log\left(\sqrt{(17.5)^2 - 35z + g} + (17.5 - z)\right) \right]$$

$$\left. - \left[\log \left(\sqrt{(-17.5)^2 + 35z + g} - (17.5 - z) \right) \right] \right\} = \frac{1}{2} \left\{ (l - z) \sqrt{l^2 - 2zl + g} \right.$$

$$\left. + (g - z^2) \left[\log \left(\sqrt{l^2 - 2zl - g} + (l - z) \right) \right] \right\}_{-17.5}^{z}$$

$$= \frac{1}{2} \left\{ (g - z^2) \left[\log \left(\sqrt{(g - z^2)} + (17.5 + z) \right) \sqrt{(17.5)^2 + 35z + g} \right] \right.$$

$$\left. - (g - z^2) \left[\log \left(\sqrt{(17.5)^2 + 35z + g} - (17.5 + z) \right) \right] \right\} .$$

The result is quite evidently not a simple expression and the integral is not easily evaluated even with series expansion. If we take into account the trapping efficiency, the problem becomes even more unmanageable. In addition, we may add terms for field lines not parallel to the z-axis and differential trapping in r; then to finally obtain a distribution in θ we must integrate between set limits of θ_0.

Monte Carlo simulation is an alternate approach to direct numerical integration. This approach has been taken primarily for its intuitive clarity and for the necessity of linking this code to the code that calculates the signal at the detectors. (Approximation of signal strength is far more easily approached stochastically then by direct integration.)

The code ANGLE (see printout and Table A1 at end of section) is used to calculate injected angular distribution. ANGLE (as well as FOIL and MEASURE) may be accessed under user number [30, 3005] on the PDP-10. It is set up to calculate distribution for 100,000 particles. The aim of the injectors is at $z_0 = 0$.

Particles are injected by first choosing an injection position on the source (via a random number). The trajectory is then chosen from a Gaussian distribution and the algorithm used to generate this distribution is Gaussian R.N. = $(-2 \ln \text{R.N.1})^{1/2} \cos 2\pi$ (R.N.2) where R.N.1 and R.N.2 are distinct random numbers.

Particles are captured on the z-axis but are weighted for capture by the measured exponential density in z; this ensures that the cross-section value is a linear function of n(z).

Distribution in z is calculated by counting particles captured along each centimeter of a 100-cm segment of the z axis centered at z = 0. Average injection angle is also calculated (Table A1). Angular distribution at the machine center is calculated by weighting the distribution of all particles by the relative time spent at the center in relation to a total period (see Experimental Analysis section).

Calculated data plots include density of injection vs z (Fig. A2), angular injection distribution (Figs. A3 and A4), and average distribution angle vs β (Fig. A5).

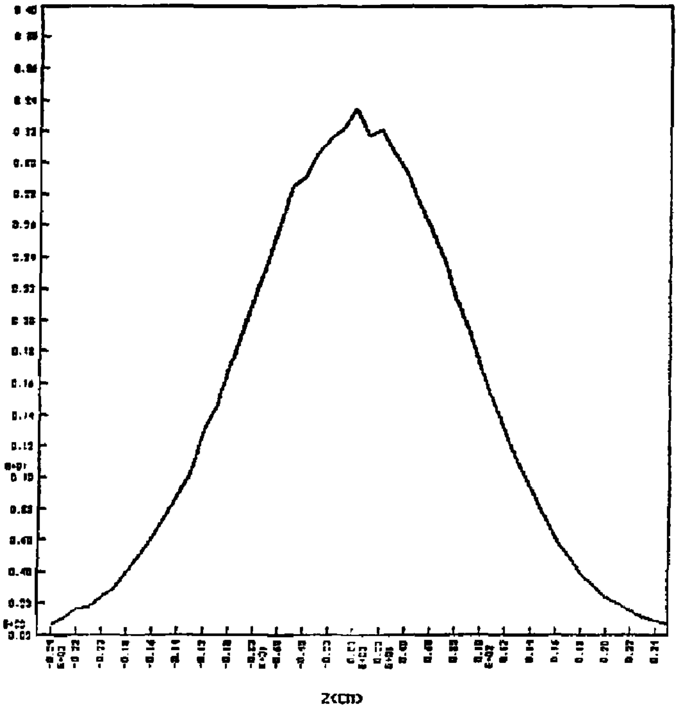

Fig. A2. Injected distribution vs z.

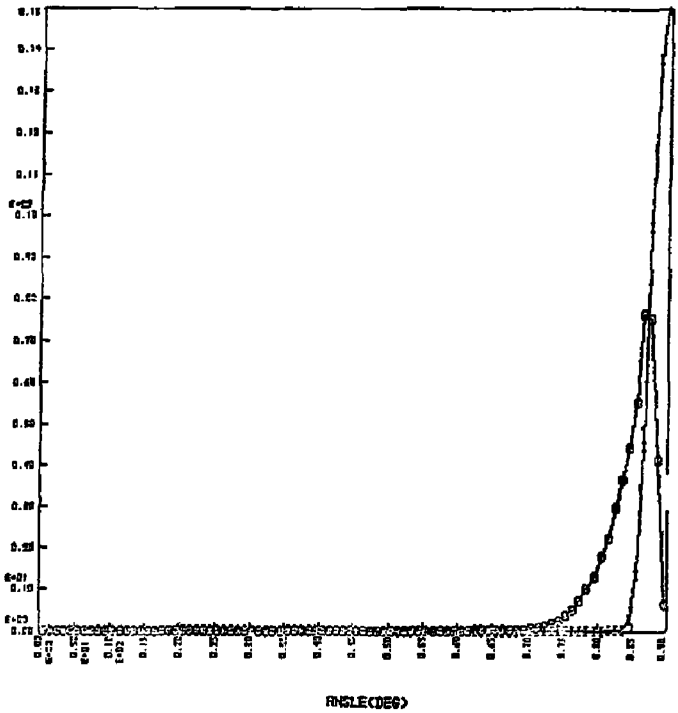

Fig. A3. Injected and center-angle distributions vs θ.

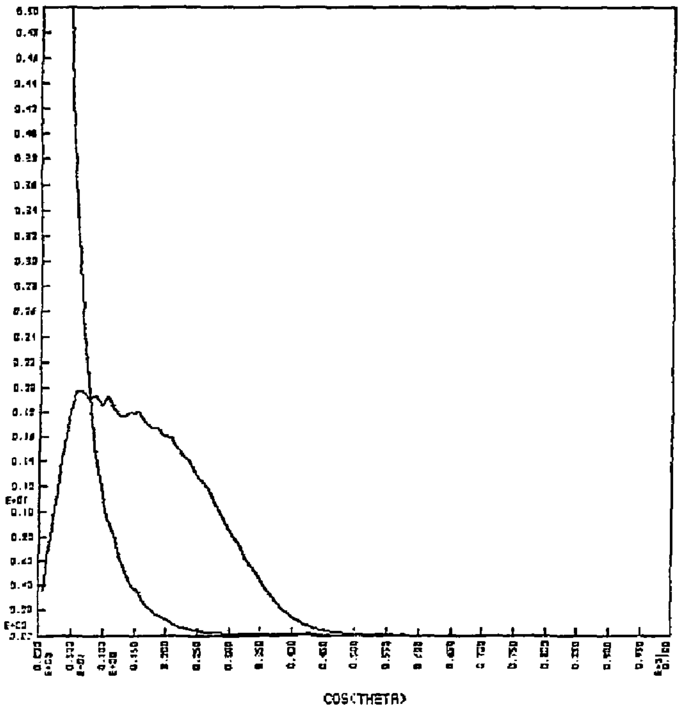

Fig. A4. Injected and center-angle distributions vs μ.

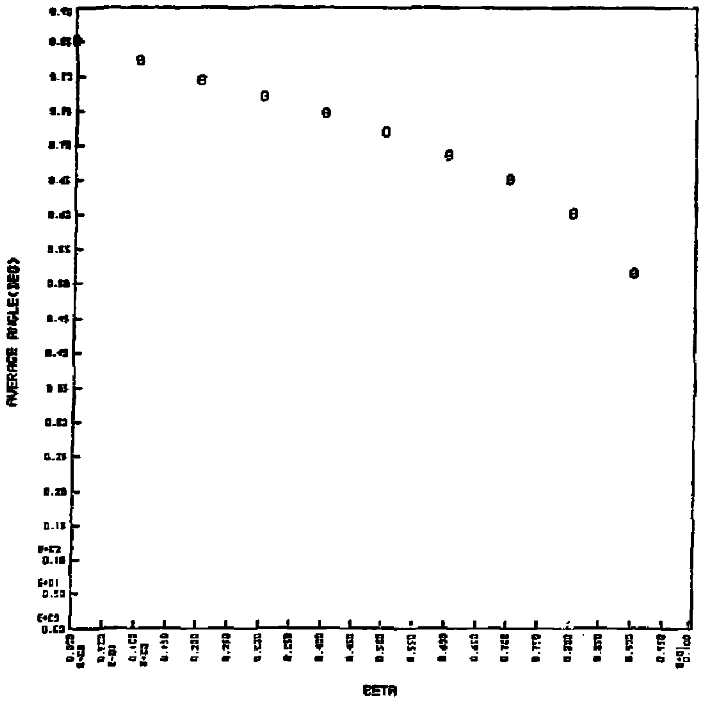

Fig. A5. Average center angle vs β.

Code ANGLE

```
C ANGLE IS DESIGNED TO CALCULATE THE INJECTED ANGULAR DISTRIBUTION OF THE 2XIIB.
C ANGLE SIMULATES INJECTION OF PARTICLES FROM THE NEUTRAL INJECTORS,
C SUBSEQUENT CAPTURE ON THE Z-AXIS, AND "TIME-AVERAGES" THE
C RESULTANT CENTER ANGLE DISTRIBUTION.  THE PROGRAM ALLOWS CALCULATION OF
C DISTRIBUTIONS AT DIFFERING BETAS, SOURCE POSITIONS, AND NUMBERS OF INJECTED
C PARTICLES.  OUTPUT INCLUDES DISTRIBUTION VS. ANGLE,Z, OR COS(THETA) AND
C AVERAGE ANGLE VS. BETA.  IN ADDITION A FILE CALLED ANGI IS CREATED TO
C OUTPUT AVERAGE INJECTION ANGLE, AVERAGE CENTER ANGLE, NUMBER OF PARTICLES IN
C THE LOSS CONE, AND DISTRIBUTION CENTER ANGLE.  THIS
C FILE CAN THEN BE READ BY MEASURE .

      DIMENSION Z(51),THC(90),THI(90),ANGLE(90),ZN(51),TMU(100),
     C ANMU(100),BTH(11),BET(11),R(2),TITLE(10),NDIST(11)
      CALL DDCOID(SHSMITH,SHBRUCE)
      CALL DDERS(1)
      DATA(TITLE(I),I=1,16)/'ANGLE(DEG)Z(CM)COS(THETA)BETA AVERAGE ANG
     CLE(DEG)   '/,(NDIST(I),I=1,11)/1.0,0,1.0,0,0.0,0.0,0/
C DISTB IS THE DESIRED BETA AT WHICH ONE WISHES TO CALCULATE CENTER ANGLE DISTRIBUTION
C FOR OUTPUT TO MEASURE.
      DISTB=.3
      DO 1 I=1,11
C BETA IS THE VALUE AT WHICH THE AVERAGE ANGLE IS CALCULATED TO PLOT AVERAGE
C CENTER ANGLE VS. BETA.
      BETA=(I-1)/10.
      BET(I)=BETA
      N=10000
C THE IF STATEMENT DETERMINES THE NUMBER OF ITERATIONS (OR PARTICLES
C   INJECTED) FOR EACH BETA. GENERALLY FOR A SPECIFIC DISTRIBUTION WE WILL DESIRE
C MORE ITERATIONS AND THEREFORE MORE ACCURACY WHILE FOR CALCULATIONS OF AVERAGES
C REQUIRES FEWER ITERATIONS.
      IF(NDIST(I).EQ.1) N=100000
      CALL A(Z,THC,THI,ANGLE,ZN,TMU,ANMU,DISTB,
     C N,BETA,THCAV)
      IF(I.GT.1) GO TO 3
C FOLLOWING PLOTS NORMALIZED DISTRIBUTIONS OF
C INJECTED AND CENTER ANGLES.
      CALL MAPS(0.0,90,0,0,0,15.0)
      CALL TRACEC(1HI,ANGLE,THI,90)
      CALL TRACEC(1HC,ANGLE,THC,90)
      CALL SETLCH(42.0,-1.7,0,0,2)
      CALL CRTBCD(TITLE(1),2)
      CALL FRAME
C Z DISTRIBUTION OF INJECTED PARTICLES.
      CALL MAPS(-25.0,25.0,0.0,4.0)
      CALL TRACE(ZN,Z,51)
      CALL SETLCH(-2.0,-.4,0,0,2)
      CALL CRTBCD(TITLE(3),1)
      CALL FRAME
C COS(THETA) DISTRIBUTION FOR CENTER.
      CALL MAPS(0.0,1.0,0.0,5.0)
      CALL SETLCH(.45,-.5,0,0,2)
      CALL CRTBCD(TITLE(4),2)
3     IF(NDIST(I).EQ.0) GO TO 1
      CALL TRACE(ANMU,TMU,100)
1     BTH(I)=THCAV
C AVERAGE CENTER ANGLE VS. BETA.
      CALL FRAME
      CALL MAPS(0.0,1.0,0.0,90.0)
      CALL POINTC(1HO,BET,BTH,11)
      CALL SETLCH(.43,-2.0,0,0,2)
      CALL CRTBCD(TITLE(6),1)
      CALL SETLCH(-.1,33.0,0,0.2,1)
      CALL CRTBCD(TITLE(7),4)
      CALL PLOTE
      CALL EXIT
      END
```

```
C A SIMULATES ACTUAL INJECTION OF PARTICLES AND THEN CALCULATES NORMALIZED
C DISTRIBUTIONS.
         SUBROUTINE A(Z,THC,THI,ANGLE,ZN,TMU,ANMU,DISTB,
     C   N,BETA,THCAV)
         DIMENSION Z(51),THC(90),THI(90),ANGLE(90),ZN(51),TMU(100),
     C   ANMU(100),CTH(11),BET(11),R(2)
C CONE IS THE LOSS CONE AT THAT BETA.
         CONE=(180./3.14)*(ASIN(SQRT(((1.-BETA)+1.E-9)/2.)))
C SC IS THE SOURCE CENTER,R IS SOURCE RADII.
         SC=0.0
         NC=0
         NI=0
         NLC=0
         THCAV=0
         AMUAV=0.0
         THIAV=0
         DRAD=180./3.14
         R(1)=213
         R(2)=370
C THC AND THI ARE THE CENTER AND INJECTED ANGLE DISTRIBUTIONS RESPECTIVELY.
         DO  11 I=1,90
         ANGLE(I)=I-.5
         THC(I)=0
11       THI(I)=0
C TMU IS THE DISTRIBUTION FOR COS(THETA) AT THE CENTER.
         DO 21 I=1,100
         TMU(I)=0.0
21       ANMU(I)=I/100.-.005
         DO 12 I=1,51
12       Z(I)=0
         DO 10 I=1,N

C GAUSSIAN DISTRIBUTION FOR SOURCE INJECTION ANGLE.
1        THZ=3.0*SQRT(-2.LOG(RAN(X)))*COS(6.283*RAN(X))

         IF(ABS(THZ)-90) 2,1,1
C S IS THE PARTICLE POSITION ON THE SOURCE BEFORE INJECTION.
2        S=RAN(X)*35.0+(SC-17.5)
         J=IFIX(RAN(X)*2.)+1.0
         RP=R(J)
C THT IS THE ANGLE BETWEEN THE SOURCE AND TARGET POSITIONS.
         THT=-ATAN((-S0+S)/RP)*DRAD
C THIAN AND THIA ARE ANGLES OF INJECTION.
         THIAN=90.0-(THZ+THT)
         THIA=90-ABS(THZ+THT)
         IF(THIA) 1,3,3
3        NI=NI+1
         THIAV=THIAV+(THIA-THIAV)/NI
C PARTICLE POSITION AT Z-AXIS.
         ZP=S+RP*COSD(THIAN)/SIND(THIAN)
         J=IFIX(ZP+25.5-S0)
         IF(J) 9,9,18
18       IF(J-51) 8,8,9
8        Z(J)=Z(J)+1
C CAP IS DENSITY VARIATION IN Z.
9        CAP=EXP(-ABS(ZP/18.5))
C THE PARTICLE IS CAPTURED ON THE Z-AXIS IF ITS PROBABILITY FOR CAPTURE IS EXCEEDED.
C THIS WEIGHTS THE CAPTURE BY LOCAL DENSITY AS WOULD BE EXPECTED.
         IF(CAP-RAN(X)) 1,7,7
C CALCULATE LOCAL B FIELD.
7        B=SQRT(((1.+(ABS(ZP)/75.)**2)**2-BETA*CAP)/((1.-BETA)+1.E-9))
         ARG=(SQRT(1/B))*SIND(THIA)
C CALCULATE ANGLE OF PARTICLE AT Z=0.
         THCA=ASIN(ARG)*DRAD
C REJECT IF IN LOSS CONE.
         IF(THCA-CO.5) 4,4,5
4        NLC=NLC+1
         GO TO 1
5        THCAV=THCAV+(THCA-THCAV)/I
         J=IFIX(THIA)+1
```

```
        THI(J)=THI(J)+1
        J=IFIX(THC9+.5)
        THC(J)=THC(J)+1
        AMU=COSD(THIA)
        J=IFIX(AMU*100.)+1
        TMU(J)=TMU(J)+1.
        AMUAV=AMUAV+(AMU-AMUAV)/I
10      NC=NC+1
        AMUAV=ACOS(AMUAV)*DRAD
C IF BETA IS THE BETA SPECIFIED IN DISTB AVERAGES . DISTRIBUTIONS ARE
C WRITTEN INTO ANGI.
        IF(BETA.NE.DISTB) GO TO 14
        OPEN(UNIT=01,ACCESS='SEQOUT',FILE='ANGI')
        WRITE(01,13)THIAV,AMUAV,THCAV,NLC,
     C  (ANGLE(K),THC(K),K=1,90)
        CLOSE(UNIT=01,ACCESS='SEQIN',FILE='ANGI')
        IF(BETA.EQ.DISTB) TYPE 600
600     FORMAT(1X,3HOK2)
13      FORMAT(//////////,1X,6HTHIAV=,F10.5,10X,6HAMUAV=,F10.5,
     C  10X,6HTHCAV=,F10.5,3X,4HNLC=,I6,///,
     C  18(/,(5(1X,4HTHC(,F4.1,2H)=,F10.3,4X))))
C THE REMAINDER OF THE ROUTINE NORMALIZES THE DISTRIBUTIONS OBTAINED.
14      AV=2.*N/90.
        AVZ=N/51.0
        AVMU=2.*N/100.0
        DO 15 I=1,90
        THC(I)=THC(I)/AV
15      THI(I)=THI(I)/AV
        RAD90=3.14/2.
        THCTOT=0.0
        ZP=0.5
C THIS DO LOOP TIME AVERAGES THE DISTRIBUTION BY CALCULATING THE TIME SPENT IN
C THAT CELL IN RELATION TO A TOTAL PERIOD.
        DO 22 I=1,100
        IF(TMU(I).EQ.0.) GO TO 22
        ANGN=ACOS(AMU(I))
        ZMAX=75.*COS(ANGN)/(SIN(ANGN))
        FTIME=1.
        IF(ZMAX.GT.ZP) FTIME=(ASIN(ZP/ZMAX))/RAD90
24      TMU(I)=TMU(I)*FTIME
22      THCTOT=THCTOT+TMU(I)

        AVMU=2.*THCTOT/100.
        DO 23 I=1,100
23      TMU(I)=TMU(I)/(AVMU)
        DO 20 I=1,51
        FZ=Z(I)/NI
        ZP=I-(IFIX(90)-25)
        Z(I)=FZ*NI/AVZ
20      ZN(I)=ZP
        RETURN
        END
```

Table A1. Center angle vs θ (THC (θ)).

THIAV= 88.23511 AMUAV= 77.19280 THCAV= 77.09345 NLC= 0

THC(0.5)=	0.000	THC(1.5)=	0.000	THC(2.5)=	0.000	THC(3.5)=	0.000	THC(4.5)=	0.000
THC(5.5)=	0.000	THC(6.5)=	0.000	THC(7.5)=	0.000	THC(8.5)=	0.000	THC(9.5)=	0.000
THC(10.5)=	0.000	THC(11.5)=	0.000	THC(12.5)=	0.000	THC(13.5)=	0.000	THC(14.5)=	0.000
THC(15.5)=	0.000	THC(16.5)=	0.000	THC(17.5)=	0.000	THC(18.5)=	0.000	THC(19.5)=	0.000
THC(20.5)=	0.000	THC(21.5)=	0.000	THC(22.5)=	0.000	THC(23.5)=	0.000	THC(24.5)=	0.000
THC(25.5)=	0.000	THC(26.5)=	0.000	THC(27.5)=	0.000	THC(28.5)=	0.000	THC(29.5)=	0.000
THC(30.5)=	0.000	THC(31.5)=	0.000	THC(32.5)=	0.000	THC(33.5)=	0.000	THC(34.5)=	0.000
THC(35.5)=	0.000	THC(36.5)=	0.000	THC(37.5)=	0.000	THC(38.5)=	0.000	THC(39.5)=	0.000
THC(40.5)=	0.000	THC(41.5)=	0.000	THC(42.5)=	0.000	THC(43.5)=	0.000	THC(44.5)=	0.000
THC(45.5)=	0.000	THC(46.5)=	0.000	THC(47.5)=	0.000	THC(48.5)=	0.000	THC(49.5)=	0.000
THC(50.5)=	0.000	THC(51.5)=	0.000	THC(52.5)=	0.000	THC(53.5)=	0.000	THC(54.5)=	2.000
THC(55.5)=	2.000	THC(56.5)=	5.000	THC(57.5)=	7.000	THC(58.5)=	20.000	THC(59.5)=	34.000
THC(60.5)=	76.000	THC(61.5)=	176.000	THC(62.5)=	239.000	THC(63.5)=	415.000	THC(64.5)=	661.000
THC(65.5)=	1003.000	THC(66.5)=	1381.000	THC(67.5)=	2013.000	THC(68.5)=	2654.000	THC(69.5)=	3426.000
THC(70.5)=	4980.000	THC(71.5)=	4843.000	THC(72.5)=	5497.000	THC(73.5)=	6012.000	THC(74.5)=	6403.000
THC(75.5)=	6572.000	THC(76.5)=	6731.000	THC(77.5)=	6674.000	THC(78.5)=	6329.000	THC(79.5)=	6019.000
[illegible]	5742.000	THC(81.5)=	5002.000	THC(82.5)=	4436.000	THC(83.5)=	4094.000	THC(84.5)=	3336.000
THC(85.5)=	2741.000	THC(86.5)=	2043.000	THC(87.5)=	1031.000	THC(88.5)=	294.000	THC(89.5)=	7.000

APPENDIX B

FOIL

We desire to calculate foil temperatures both to predict signal strengths of the detector and to ensure that the foils don't melt. The heating and cooling of the foils, however, is essentially a nonlinear process. Although we may approximate signal strengths for a given neutral flux (dV/dt) and average foil temperature (V), a detailed study of local foil temperatures and change of signal in time requires closer analysis.

FOIL (see printout at end of section) is used to calculate local foil temperatures and evolution of signal strength in time for varying neutral flux and current strengths and lifetimes. The main contributions to heating are neutral flux and ohmic heating. Contributions to cooling include radiation and conduction to the walls and center of the foil.

Each foil can be approximated by an annulus of inner diameter 0.125 in. and outer diameter 0.43 in. (Fig. 4). The coefficient of heat conduction is $k = 0.15$ cal/cm^2/cm/°C/s. The heat capacity is 0.12 cal/g over the range of temperatures considered, while the density is 8.9 g/cm^3. As noted previously, the resistivity of the nickel foil is $6.84\ [1 + 6.9 \times 10^{-3}\ (T - 20)\ (°C)]$ μ ohm cm.

Using these parameters we can calculate heat losses and gains. For radiation we have

$$\begin{aligned}
\text{RAD} &= e\ \sigma\ T^4 \\
&= (0.3 \text{ for metals}) \left(5.669 \times 10^{-5}\ \frac{\text{erg}}{\text{s cm}^2}\right) T^4\ (°\text{K}^4)\ A(\text{cm}^2) \\
&= 1.7 \times 10^{-5}\ AT^4 \text{ erg/s} \\
&= 1.7 \times 10^{-12}\ At^4\ (°\text{K}^4) \text{ J/s}\ .
\end{aligned}$$

For conduction we have

$$\begin{aligned}
\text{COND} &= KA\ \Delta T/L \\
&= (0.15 \text{ cal/cm}^2/\text{cm}/°\text{C/s})\ [10^{-4} \text{ in. thick})\ (2.54 \text{ cm/in.}) \\
&\qquad \times (\text{circumference (cm)})]\ \frac{\Delta T(°\text{C})}{L} \\
&= 0.381 \times 10^{-4}\ \Delta T\ (°\text{C})/L \text{ cal/s} \\
&= 1.6 \times 10^{-4}\ \Delta T\ (°\text{C})/L \text{ J/s}.
\end{aligned}$$

For ohmic heating we have

$$\text{Ohm} = I^2\ (\Omega L/A)$$

$$= I^2\ (A^2)\ [1 + 0.0069\ (T - 20)(°C)](6.84 \times 10^{-6}\ \text{ohm cm})L(\text{cm})/(2\pi rt)(\text{cm}^2)$$

$$= I_L^2\ [1 + 0.0069\ (T - 20)(°C)]\ (6.84 \times 10^{-6})\ (2\pi r)(2.54 \times 10^{-4})\ \text{J/s}.$$

and, for flux heating we have

FLUX = (flux in J)(area).

Foil divides the foil into 100 annular rings of constant annular width; each ring is then treated linearly for small time intervals. During each time interval, a change in temperature is calculated by computing the heat losses and gains and then dividing by the heat capacity of that ring. Conduction is computed between adjacent rings and voltage is computed as the series voltage of concentric rings.

Turning the flux on and off simulates plasma lifetime. Current duration may also be varied to simulate finite relay-contact times. Graphics includes temperature vs radius (Figs. B1–B3), maximum temperature vs time (Fig. B4), and voltage (Fig. B5) and dv/dt vs time (Fig. B6).

Initial runs utilizing plasma lifetimes of 10 ms, flux of 100 W/cm^2, and currents of 1–10 A show the signals to be adequate and the temperatures to be well below melting (Figs. B1-B6, I = 3 A). Within the expected operating parameters, the program demonstrates clearly that the signal is almost totally linearly dependent upon the flux. We need not be concerned with competition from ohmic heating or cooling processes which would damp out the desired signal.

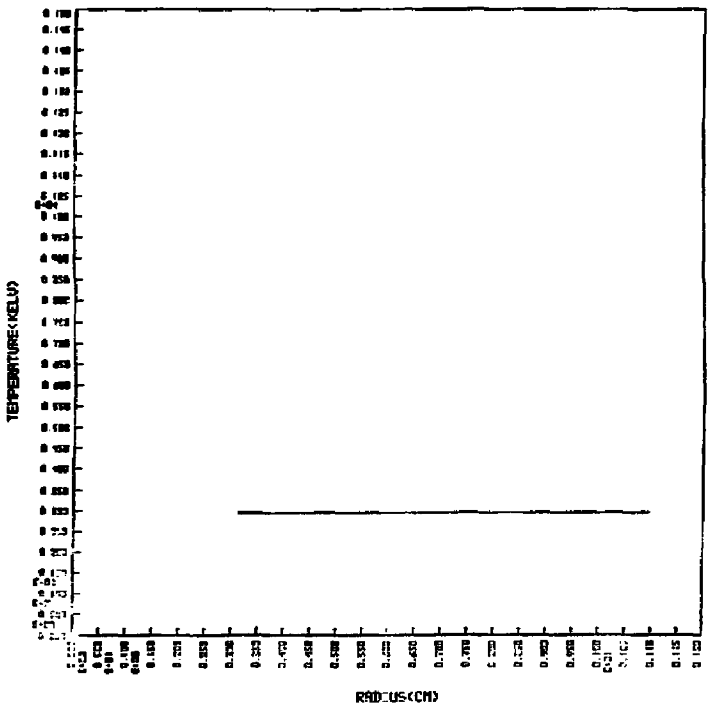

Fig. B1. Temperature vs radius before flux.

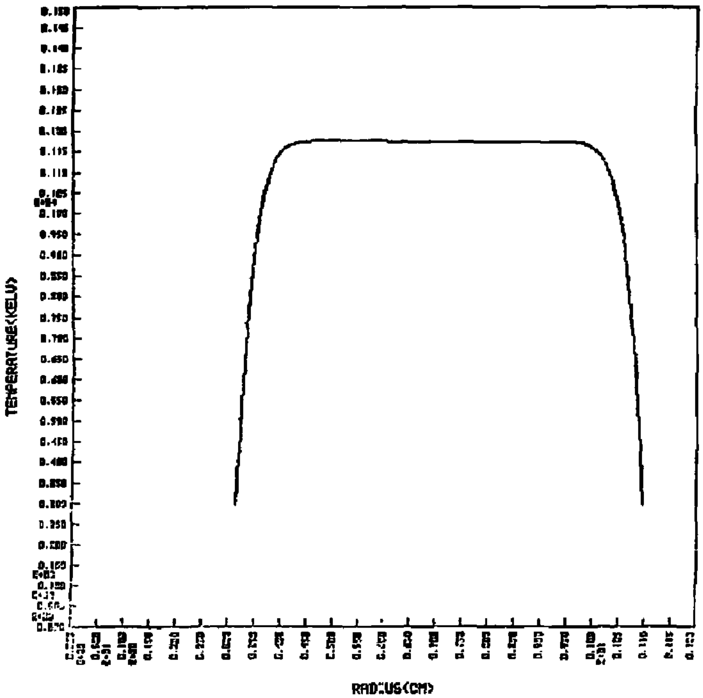

Fig. B2. Temperature vs radius during flux.

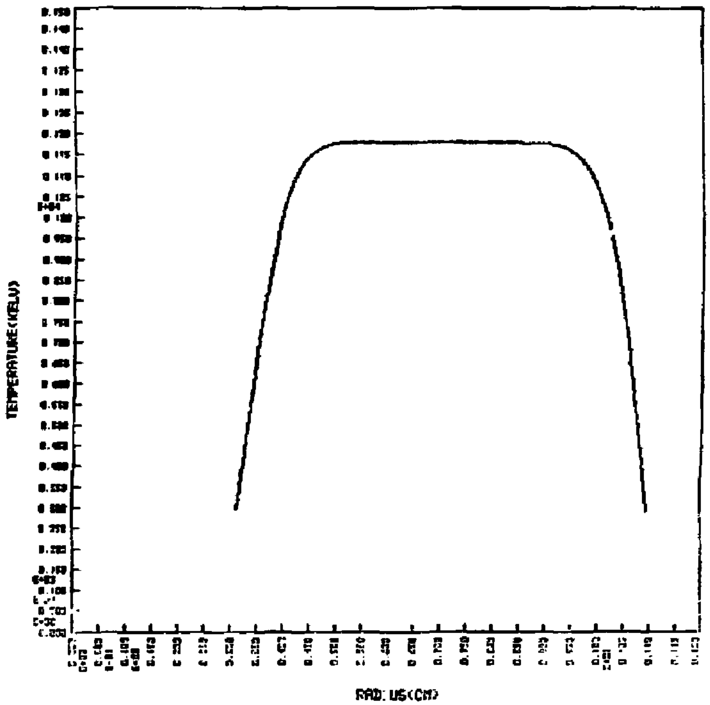

Fig. B3. Temperature vs radius upon current turnoff.

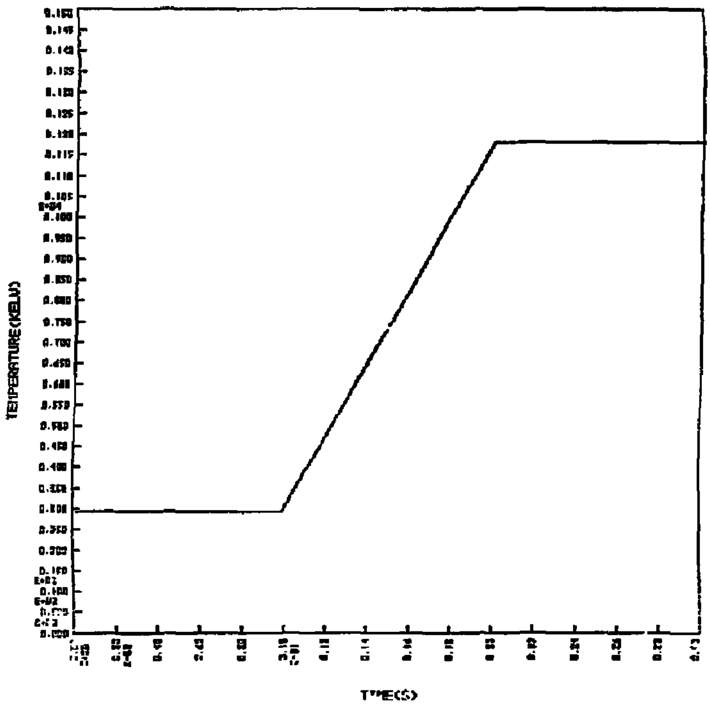

Fig. B4. Maximum temperature vs time.

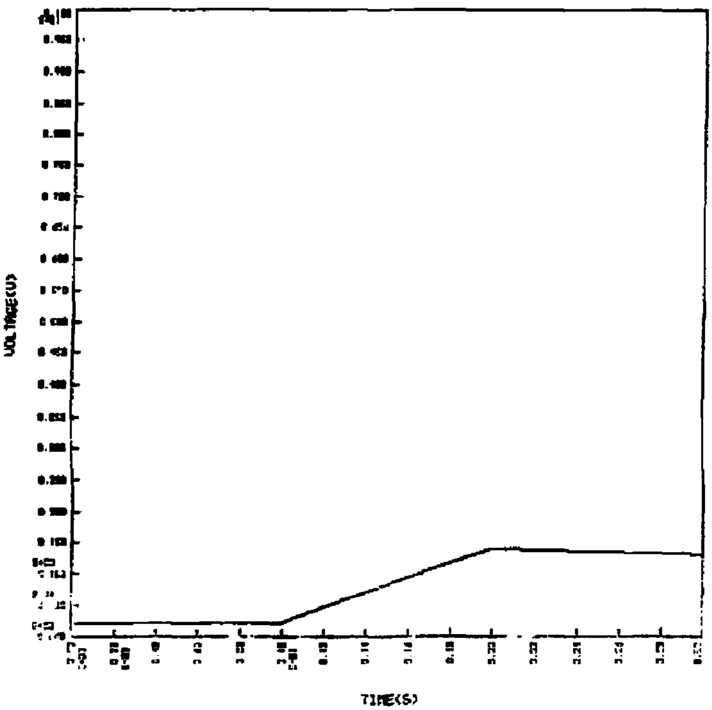

Fig. B5. Voltage vs time.

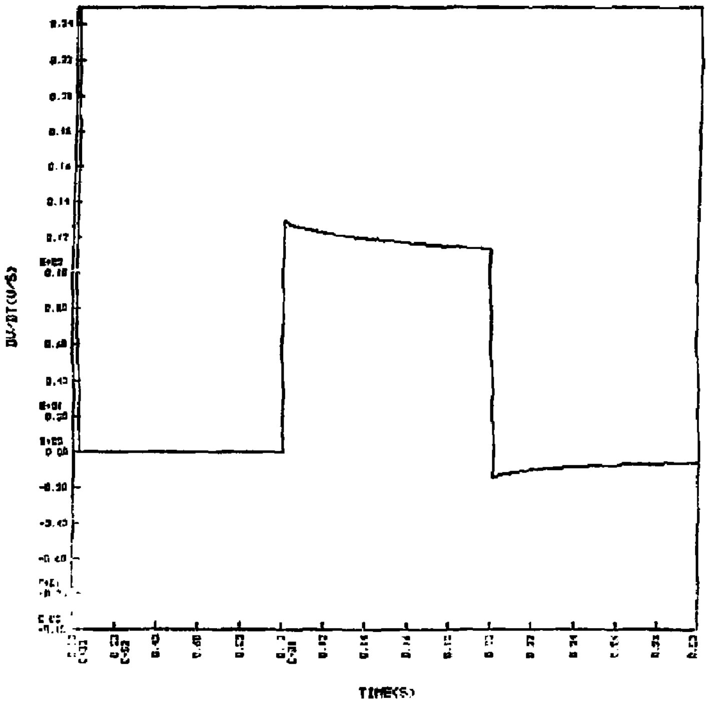

Fig. B6. dV/dt vs time.

Code FOIL

```
C FOIL CALCULATES THE TEMPERATURE AND SIGNAL AT THE FOILS OF THE DETECTORS.
C IT MAY PLOT MAXIMUM TEMPERATURE VS. RADIUS AS WELL AS TEMPERATURE AND SIGNAL
C VS. TIME.  THERE ARE PROVISIONS FOR VARYING PLASMA LIFETIME AS WELL AS CURRENT
C DURATIONS.
         DIMENSION T(102),TNEW(102),R(102),VOLT(300),ASIDE(102),
      C  DVDT(300),N1(3),N2(3),ON(3),OHM(102),
      C  TM(300),TIME(300),TITLE(12)
         DATA(TITLE(I),I=1,12)/'TEMPERATURE(KELV)    RADIUS(CM)TIME(S)    VOL
      CTAGE(V)DV/DT(V/S)'/
         DATA(N1(K),N2(K),ON(K),K=1,3)/1,100,0.,101,200,1.,201,300,0./
         CALL DD00ID(5HBRUCE,5HSMITH)
         CALL DDERS(I)
C DR IS THE WIDTH OF EACH ANNULAR RING.
         DR=(.43-.125)*2.54/100.
C SPECIFIC HEAT FOR NICKEL.
         CPV=.12*8.9*4.18
         T0=293.
         RIN=.125*2.54
         RAD360=2.*3.14
C TH IS FOIL THICKNESS.
         TH=.0001*2.54
         RESC=(1.-293.*.0069)
C HK IS THE CONDUCTION COEFFICIENT FOR NICKEL.
         HK=.15*4.18/DR
         RES=6.84E-6
         RAD=-1.7E-12/(TH*CPV)
         COND=HK/(CPV*DR)
         FLUX=100./(TH*CPV)
         DO 7 I=1,102
C ANNULAR RADIUS FROM FOIL CENTER.
         R(I)=RIN+(I-1.5)*DR
C ASIDE(I) IS THE EDGE AREA OF AN ANNULAR RING OF THE FOIL.
         ASIDE(I)=R(I)*RAD360*TH
 7       OHM(I)=RES/((ASIDE(I)**2)*CPV)
C THIS PROGRAM ITERATES FOR DESIRED VALUES OF THE CURRENT.
         DO 9 CUR=1.,10.,3.
         CUR2=CUR**2
         TAU=0.
         V0=0.
         DO 8 I=1,102
         T(I)=T0
8        TNEW(I)=T0
         DO 4 K=1,3
C DTAU IS THE TIME INTERVAL BETWEEN MEASUREMENTS OF FOIL PARAMETERS.
         DTAU=1.E-4
         DO 1 I=N1(K),N2(K)
         TAU=TAU+DTAU
         V=0.0
         CURNT=CUR
         L=K
C HEAT CALCULATES TEMPERATURE AND SIGNAL OF
C EACH RING DURING EACH ITERATION.
         CALL HEAT(V,DV,TMAX,TAU,R,CPV,T,TNEW,T0,V0,CURNT,DR,DTAU,ON,
      C  L,CUR2,OHM,COND,FLUX,RESC,RES,RAD,ASIDE)
C THESE ARE VALUES OF DV/DT, V, AND MAXIMUM TEMPERATURE (TM) IN TIME.
         DVDT(I)=DV
         TM(I)=TMAX
         TIME(I)=TAU
1        VOLT(I)=V
C PLOT TEMPERATURE VS. RADIUS.
         CALL MAPS(0.,1.2,0.,1500.)
         CALL TRACE(R,T,102)
         CALL SETLCH(.55,-150.,0,0,2,0)
         CALL CRTBCD(TITLE(5),2)
         CALL SETLCH(-.12,525.,0,0,2,1)
         CALL CRTBCD(TITLE(1),4)
```

```
4        CALL FRAME
C PLOT MAXIMUM TEMPERATURE VS. TIME.
6        CALL MAPS(0.0,.030,0.0,1500.)
         CALL TRACE(TIME,TM,300)
         CALL SETLCH(.014,-150.,0,0,2,0)
         CALL CRTBCD(TITLE(7),2)
         CALL SETLCH(-.003,525.,0,0,2,1)
         CALL CRTBCD(TITLE(1),4)
         CALL FRAME
C PLOT VOLTAGE VS. TIME.
         CALL MAPS(0.,.03,0.,1.0)
         CALL TRACE(TIME,VOLT,300)
         CALL SETLCH(.014,-.10,0,0,2,0)
         CALL CRTBCD(TITLE(7),2)
         CALL SETLCH(-.003,.45,0,0,2,1)
         CALL CRTBCD(TITLE(9),2)
         CALL FRAME
C PLOT DV/DT VS. TIME.
         CALL MAPS(0.,.03,-10.,25.)
         CALL TRACE(TIME,DVDT,300)
         CALL SETLCH(.014,-13.5,0,0,2,0)
         CALL CRTBCD(TITLE(7),2)
         CALL SETLCH(-.003,6.0,0,0,2,1)
         CALL CRTBCD(TITLE(11),2)
9        CALL FRAME
         CALL PLOTE
         CALL EXIT
         END
         SUBROUTINE HEAT(V,DV,TMAX,TAU,R,CPV,T,TNEW,T0,V0,CURNT,DR,DTAU,ON,
     C   L,CUR2,OHM,COND,FLUX,RESC,RES,RAD,ASIDE)
         DIMENSION T(102),TNEW(102),R(102),VOLT(300),ASIDE(102),
     C   DVDT(300),N1(3),N2(3),ON(3),OHM(102),
     C   TM(300),TIME(300)
         DO 1 I=2,101
C THIS STATEMENT DETERMINES NET TEMPERATURE GRADIENT BETWEEN ADJACENT ANNULI.
         DT=2.*T(I)-T(I-1)-T(I+1)
         T(I-1)=TNEW(I-1)
C AVERAGE TEMPERATURE BETWEEN TIME INTERVALS.
         TAV=(T(I)+TNEW(I))/2.
         TNEW(I)=(-RAD+ON(L)*FLUX-COND*DT+CUR2*OHM(I)*(RESC+.0069*TAV))
     C   *DTAU+T(I)
         V=V+CURNT*(RESC+.0069*TNEW(I))*DR*RES/ASIDE(I)
         IF(TNEW(I).GT.TNEW(I-1)) TMAX=TNEW(I)
  1      CONTINUE
         DV=(V-V0)/DTAU
         V0=V
         T(101)=TNEW(101)
         RETURN
         END
```

APPENDIX C

MEASURE

To approximate the signals at the foils from the charge-exchange products, we treated the plasma center as a point source. Charge exchange, in reality, occurs throughout the plasma, and an injected particle may ultimately result in a secondary or tertiary (or greater) product being received at the detector. Since we now have a volume source, the collimator will block part of the signal normally seen by the detector.

We must then determine how much of the signal reaches our detector and, more importantly, whether the detector measures a proportionate signal at each foil in relation to the angular distribution of the plasma. MEASURE can provide these answers.

MEASURE (see printout and Table C1 at end of section) may obtain its center-angle distribution by reading ANGLE's output file or, alternatively, the distribution may be directly input by equation. The distribution is then time averaged as it was for ANGLE; however, the time-averaging subroutine of MEASURE has an additional capability for graphing relative density vs (Fig. C1). One would expect this output to result in a dependence, as calculated by microwave measurements. Therefore, we can check our angular distribution by simply comparing computer-generated z-density and microwave measurements. The dependence is exponential as expected.

The subroutine DETECT follows the injected particle through rather complicated geometrical steps until its final capture or rejection by the detector. The position of the particle is initially chosen by random number from an array specifying the 12 source locations of 2XIIB plasma. Position in z and injection angle are then randomly chosen as they were in ANGLE. The particle is then "moved" to ρ = 15 cm (the plasma outer boundary) by transfer from initial to final positions in spherical coordinates ($x = x_0 + r \cos\theta \sin\phi$, etc.).

The particle is advanced in 1-cm steps at the plasma boundary until it charge exchanges (or leaves the plasma). A probability of charge exchange is randomly chosen, then the charge-exchange integral is calculated at each step by letting

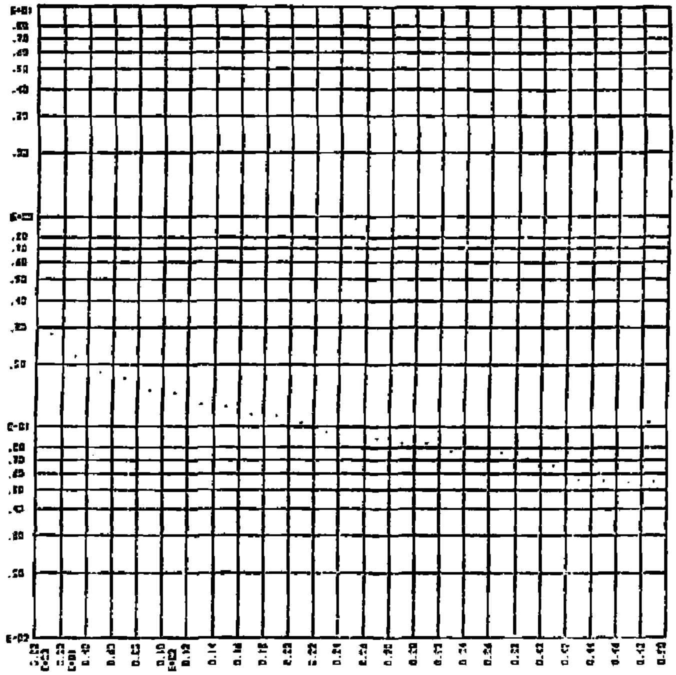

Fig. C1. Collimation simulation.

$$\text{CXINT} = \int_{\rho_1}^{\rho_2} \int_{z_1}^{z_2} e^{-\left(\frac{\rho}{735}\right)^2} e^{-\left(\frac{z}{17}\right)} \, d\rho dz \approx e^{-\left(\frac{\rho}{735}\right)} e^{-\left(\frac{z}{17}\right)} \, dr$$

so that the probability of charge exchange is

$$\text{PCX} = 1. - e^{-\left(\frac{\text{CXINT}}{7.71}\right)}$$

and the mean free path is $\lambda = 7.71$ cm. The mean free path has been calculated from Ref. 5 for a deuterium plasma of $n_0 \approx 1.2 \times 10^{14}$, $\langle E \rangle_{ion} \approx 9$ keV and $\langle E \rangle_{beam} \approx 14.7$ keV. We have an interaction rate of 1.25×10^{-7} cm^3/s and the velocity of each beam particle is now

$$\langle v \rangle = \sum_i f_i \sqrt{\frac{2E_i}{m}}$$

$$= \sum_i f_i \sqrt{\frac{2E_i(\text{keV})\ (10^3\ \text{eV/keV})\ (1.6 \times 10^{-19}\ \text{J/eV})}{(2 \times 1.67 \times 10^{-27}\ \text{kg})}}$$

$$= 3.1 \times 10^5\ (0.5\ \sqrt{20} + 0.4\ \sqrt{10} + 0.1\ \sqrt{6.7})$$

$$= 1.16 \times 10^6\ \text{m/s}$$

$$\lambda = \left(\frac{v}{\text{interaction rate x n}}\right)$$

$$= \left[\frac{1.16 \times 10^6\ \text{m/s}}{(1.25 \times 10^{-7}\ \text{cm}^3/\text{s})(1.2 \times 10^{14}\ \text{cm}^{-3})}\right]$$

$$= 0.0771\ \text{m}$$

$$= 7.71\ \text{cm}.$$

When a charge exchange takes place a new θ and ϕ are chosen to reflect the charge exchange of the parent ion; θ is chosen from the angular distribution and ϕ is randomly chosen. The new coordinates of the charge exchange are used as new initial coordinates, and the process of "stepping" through the plasma is again repeated until the particle leaves the plasma without charge exchange.

The particle is determined to have left the plasma when it reaches the spherical radius of the foil from plasma center. To simulate collimation (Fig. C2), two critical tests must be passed. First, the particle is moved along its trajectory until it is within 0.01 cm of the foil. Next, the detector is chosen on the basis of whether the θ of the particle is within $\pm 7.5°$ that of a detector. As $7.5°$ is greater than the maximum acceptance angle of the collimated detectors $\left(\arcsin \frac{0.43 \text{ in. radius}}{4 \text{ in. collimator}} = 6.17 \right)$, it provides a convenient cutoff between detectors (which are spread $15°$ ($\pm 7.5°$) apart).

To facilitate simulation by cutting the number of iterations, we are accepting any particle that falls in a particular angular band as a candidate for detection. In reality, the foil takes up only one small portion of the band. To simulate collimation and finite foil radius then, the foil is placed on the center line of the angular band with the foil center randomly positioned within one foil radius of the particle's projection on the center line (Fig. C2). The particle must be less than a foil radius from the foil center if it is to be captured.

In addition to stepping the particle back to the collimator top, a similar test must be passed. The particle is captured only if it passes through both the collimator top and the foil.

Preliminary runs of the MEASURE program, utilizing injected-ion distribution, show that 49 out of 10,000 particles are captured in the first channel, and 9 are captured in the second channel. For an isotropic distribution and no collimation we would expect that the

$$\begin{aligned} \text{Number of particles captured} &= \frac{\text{area of band}}{\text{total area}} \times \text{number of injected particles} \\ &= \frac{2\pi(13 \text{ in.})(0.43 \text{ in.})}{4\pi(13 \text{ in.})^2} \times 10{,}000 \\ &= 165 \end{aligned}$$

so that we would obtain $\frac{49}{165} \approx 29.7\%$ isotropic in the first channel. While the signal would be less than previously estimated, it would nonetheless be quite significant.

We cannot ignore that the estimated signal at the second detector is only 1/5 that of the first detector. However, from Fig. A4 we would expect the two signals to be about equal. (The signal for the first channel $\approx 2\times$ (cos 84°

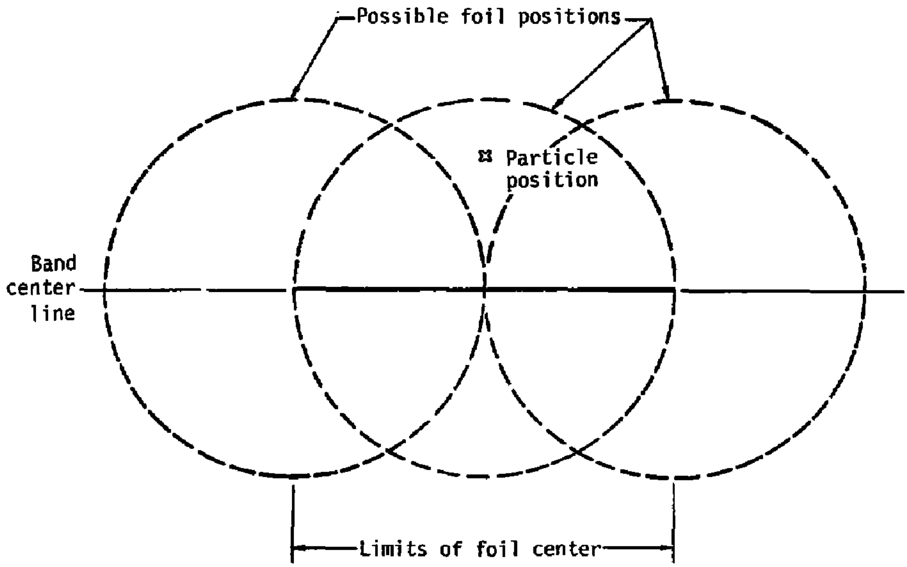

Fig. C2. Density vs z.

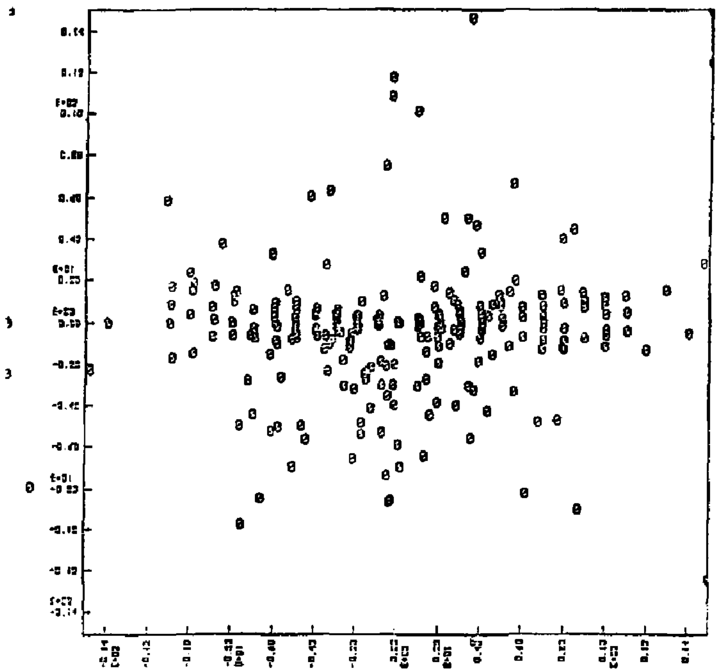

Fig. C3. Charge-exchange location at midplane.

≈ 0.21 and the signal for the second channel $\approx 1x\ (\cos 81° - \cos 69°) \approx 0.20$. The area for both bands is about equal. Therefore, we must either calibrate the signal to obtain the correct distribution or adjust the amount of calibration to obtain a more accurate direct measure.

Table C1. Number of particles detected at each detector (10,000 injected particles).

```
DETECTOR( 1)=  49
DETECTOR( 2)=   9
DETECTOR( 3)=   0
DETECTOR( 4)=   0
DETECTOR( 5)=   0
```

Code MEASURE

```
C MEASURE IS A PROGRAM DESIGNED TO SIMULATE THE CAPTURE OF NEUTRALS
C AT THE DETECTOR.  IT SUBSEQUENTLY CALCULATES THE NUMBER OF NEUTRALS
C RECIEVED AT EACH DETECTOR FOR A GIVEN ANGULAR DISTRIBUTION AT THE CENTER.
       DIMENSION THC(90),ANG(50,90),NDET(5),ANGLE(90)
       DATA(NDET(I),I=1,5)/5*0.0/
       OPEN(UNIT=21,ACCESS='SEQOUT',DISPOSE='PRINT',FILE='DTCT')
       CALL DDBOID(5HBRUCE,5HSMITH)
        DATA((ANG(M,N),M=1,50),N=1,90)/4500*0.0/
C THE FOLLOWING TWO STATEMENTS CAUSES THE FILE CREATED BY ANGLE TO
C BE OPENED AND THE DESIRED ANGULAR DISTRIBUTION TO BE READ.
       OPEN(UNIT=01,ACCESS='SEQIN',FILE='ANGI')
       READ(01,13)THIAV,AMUAV,THCAV,NLC,(ANGLE(K),THC(K),K=1,90)
       CLOSE(UNIT=01,ACCESS='SEQIN',FILE='ANGI')
       TYPE 13,THIAV,AMUAV,THCAV,NLC,(ANGLE(K),THC(K),K=1,90)
13     FORMAT(//////////,1X,6HTHIAV=,F10.5,10X,6HAMUAV=,F10.5,
     C 10X,6HTHCAV=,F10.5,3X,4HNLC=,I6,///,
     C 18(/,(5(1X,4HTHC(,F4.1,2H)=,F10.3,4X))))
C MAPS IS CALLED SO THAT A PLOT OF CHARGE EXCHANGE LOCATION CAN BE MADE.
C ANGZ "TIME-AVERAGES' THE ANGULAR DISTRIBUTION  FROM ANGLE.
       CALL MAPGSL(0.0,50.,.001,.5)
       CALL ANGZ(THC,ANG)
C DETECT SIMULATES THE INTERACTION OF INJECTED NEUTRALS, THEIR CHARGE EXCHANGE
C AND SUBSEQUENT CAPTURE AT THE DETECTOR.
       CALL FRAME
       CALL MAPS(-15.,15.,-15.,15.)
       CALL DETECT(ANG,NDET)
       PAUSE
50     FORMAT(//////////,5(/,10X,9HDETECTOR(,I2,2H)=,I4))
C WRITES A FILE CONTAINING THE NUMBER OF NEUTRALS DETECTED AT EACH OF THE FOILS.
       WRITE(21,50),(N,NDET(N),N=1,5)
5      TYPE 50,N,NDET(N)
       CALL PLOTE
       CALL EXIT
       END
       SUBROUTINE ANGZ(THC,ANG)
       DIMENSION THC(90),ANG(50,90)
       DO 1 I=1,50
       THCTOT=0.0
       NZ=I-0.5
       Z=NZ
       Z1=NZ-.5
       DO 2 N=1,90
       Z2=Z1+1.
       IF(THC(N)) 2,2,3
3      ANGN=(N-.5)*3.14/180.
C ZMAX IS THE TURN-AROUND POINT FOR MIRRORED PARTICLES WITH PITCH ANGLE ANGN.
       ZMAX=75.*COS(ANGN)/SIN(ANGN)
       IF(Z1-ZMAX) 4,2,2
4      IF(Z2>ZMAX) Z2=ZMAX
C FTIME IS THE FRACTION OF TIME SPENT IN THE CELL (Z2-Z1).
       FTIME=(2.*(ASIN(Z2/ZMAX)-ASIN(Z1/ZMAX)))/3.14
       ANG(I,N)=THC(N)*FTIME
2      THCTOT=THCTOT+ANG(I,N)
C PLOTS Z VS. THCTOT(DENSITY).
       CALL POINT(Z,THCTOT)
       DO 1 N=1,90
1      ANG(I,N)=ANG(I,N)/(THCTOT+1.E-9)
       RETURN
       END
```

```
      SUBROUTINE DETECT(ANG,NDET)
      DIMENSION R0(12,2),NDET(5),ANG(50,90),ANGD(5),RHOD(5),ZD(5)
      DATA((R0(I,J),I=1,12),J=1,2)/2*-375.66,2*-378.91,2*-380.,2*324.1
     C 2,2*327.68,2*329.76,57.26,-57.26,28.71,-28.71,2*0.,62.02,-62.02,
     C 37.36,-37.36,12.48,-12.49/,DR/1.0/,CXINT/0.0/
      PIRAD=3.14/180.
      RD=13.*2.54
C THIS DO LOOP INITIALIZES THE VALUES OF DETECTOR ANGLE, Z LOCATION AND
C DISTANCE R FROM THE Z-AXIS.
      DO 7 I=1,5
      ANGD(I)=(75+15*I)*PIRAD
      ZD(I)=RD*COS(ANGD(I))
7     RHOD(I)=RD*SIN(ANGD(I))
      RF=.43*2.54/2.
      RC=4.*2.54
      NJ=10000
      DO 10 J=1,NJ
      NUMBER=0
CHOOSE SOURCE.
      I=IFIX((12.*RAN(W))+1.0)
C X0, Y0, Z0, RHO0 SPECIFY THE INITIAL LOCATION OF THE NEUTRAL.
      X0=R0(I,1)
      Y0=R0(I,2)
      IC=0
      Z0=-27.5+35.0*RAN(W)
      RHO0=SQRT(X0**2+Y0**2)
C  THZ IS CHOSEN FROM A GAUSSIAN DISTRIBUTION AND THE PARTICLE IS
C "STEPPED" TO RHO = 15.(15 CM. FROM THE Z-AXIS.)
      PHI=ATAN2(-Y0,-X0)
      THZ=2.*SQRT(-ALOG(RAN(W)))*COS(6.283*(RAN(W)))
C THT IS THE ANGLE BETWEEN THE SOURCE POINT AND THE TARGET POINT.
      THT=ATAN2((-15.+Z0),RHO0)
      THI=(90.-(THZ+THT))*3.14/180.
      R=ABS((RHO0-15.)/SIN(THI))
      Z=Z0+R*COS(THI)
      X=X0+R*COS(PHI)*SIN(THI)
      Y=Y0+R*SIN(PHI)*SIN(THI)
C CXINT IS THE CHARGE EXCHANGE INTEGRAL WHICH MUST EXCEED THE CHARGE
C EXCHANGE PROBABILITY BEFORE THE EVENT MAY TAKE PLACE.
5     CXINT=0.0
      R0=SQRT(RHO0**2+Z0**2)
      DR=1.0
C PROBCX IS THE PROBABILITY FOR CHARGE EXCHANGE.
      PROBCX=1.-RAN(W)
C THIS LOOP "STEPS" THE PARTICLE THROUGH THE PLASMA UNTIL CHARGE EXCHANGE
OCCURS OR THE PARTICLE LEAVES THE PLASMA.
      DO 1 IC=1,100
      RHO=SQRT(X**2+Y**2)
      R=SQRT(RHO**2+Z**2)
      CXINT=CXINT+EXP(-(RHO/7.35)**2)*EXP(-ABS(Z)/17.)*DR
      PCX=1.-EXP(-CXINT/8.96)
      IF(PCX>PROBCX) GO TO 3
      IF(R>=RD.AND.(R0<RD.OR.IC>1)) GO TO 6
      X=X+DR*COS(PHI)*SIN(THI)
      Y=Y+DR*SIN(PHI)*SIN(THI)
      Z=Z+DR*COS(THI)
1     CONTINUE
C N DEFINES WHICH ANGULAR DISTRIBUTION AS A FUNCTION OF Z WE SHALL PICK.
3     N=IFIX(ABS(Z))+1
      ANGP=RAN(W)
      ANGT=0.0
C THIS LOOP CHOOSES THE N      TH ANGLE.
      DO 4 I=1,90
      ANGT=ANG(N,91-I)+ANGT
      IF(ANGT<ANGP) GO TO 4
C COMPUTE NEW INITIAL VALUES AND TRAJECTORY FOR THE NEUTRAL.
      X0=X
      Y0=Y
      Z0=Z
      RHO0=SQRT(X**2+Y**2)
```

```
      THTA=I-.5
      ARG=SQRT((1.+(Z/75.)**2)*(SIND(THTA)**2))
      IF(ARG>1.) ARG=1.
      THTA=ASIN(ARG)
      THI=3.14/2.-THTA*(1-2*IFIX(RAN(W)*2.))
      PHI=2.*3.14*RAN(W)
      GO TO 5
4     CONTINUE
C IF THIS CONDITION HOLDS WE ARE EITHER HITTING THE OPPOSITE SIDE OF THE MACHINE
C OR MISSING BY A LONG WAYS.
6     IF(ABS(R-RD)>ABS(DR)+.01) GO TO 10
C THESE STATEMENTS CAUSE THE PARTICLE TO BE STEPPED TO WITHIN .01 CM
C OF THE FOIL  RADIUS (FROM PLASMA CENTER)
      IF(R>RD) DR=-.5*ABS(DR)
      IF(R<RD) DR=.5*ABS(DR)
      X=X+DR*COS(PHI)*SIN(THI)
      Y=Y+DR*SIN(PHI)*SIN(THI)
      Z=Z+DR*COS(THI)
      R=SQRT(X**2+Y**2+Z**2)
      IF(ABS(R-RD)>.01) GO TO 6
      RHO=SQRT(X**2+Y**2)
      IF(ABS(Z0)<1.) CALL POINTC(1H0,X0,Y0)
      DO 9 I=1,5
      IF(ABS(ANGD(I)-THI)<=7.5*3.14/180.) GO TO 8
9     CONTINUE
      GO TO 10
C THE PARTICLE IS CONSIDERED TO BE CAPTURED IF IT STRIKES WITHIN A BAND OF
C THE SAME WIDTH AS THE FOIL AND WITH THE SAME ANGLE (THETA).  DELZ
C THEN PICKS THE DISTANCE FROM THIS ARBITRARY
C FOIL LOCATION. COLLIMATION CAN THEN BE COMPUTED
C AS WHETHER THE PARTICLES STRIKE WITHIN THE CIRCLE
C OF FOIL AS WELL AS THE TOP CIRCLE OF THE COLLIMATOR.
8     DEL=RF*(.5-RAN(W))
      PHID=ATAN2(Y,X)+DEL/RHO
C COMPUTE THE DIFFERENCE IN Z AND PERPENDICULAR DISTANCE FROM THE Z AXIS
C BETWEEN THE PARTICLE AND THE DETECTOR.
      DELZ=Z-ZD(I)
      DELRHO=RHO-RHOD(I)
C THESE ARE THE X AND Y COORDINATES OF THE PARTICLE AS DEFINED IN
A PLANE CONTAINING THE FOIL AND WITH THE FOIL CENTER AS THE AXIS CENTER.
      XC=DEL
      YC=SQRT(DELZ**2+DELRHO**2)*(-DELZ)/ABS(DELZ)
      IF(SQRT(XC**2+YC**2)>RF) GO TO 10
      PHI=ATAN2(Y-Y0,X-X0)
      DELPHI=PHI-PHID
      DELTHI=THI-ANGD(I)
C THESE ARE THE COORDINATES AS SPECIFIED IN THE COLLIMATOR
C TOP COORDINATE SYSTEM.
      DELX=RC*SIN(DELPHI)/COS(DELPHI)-XC
      DELY=RC*SIN(DELTHI)/COS(DELTHI)-YC
      IF(SQRT(DELX**2-DELY**2)>RF) GO TO 10
      NDET(I)=NDET(I)+1
      TYPE 16
16    FORMAT('CAPTURE')
10    CONTINUE
      RETURN
      END
```

NOTICE

This report was prepared as an account of work sponsored by the United States Government. Neither the United States nor the United States Energy Research & Development Administration, nor any of their employees, nor any of their contractors, subcontractors, or their employees, makes any warranty, express or implied, or assumes any legal liability or responsibility for the accuracy, completeness or usefulness of any information, apparatus, product or process disclosed, or represents that its use would not infringe privately-owned rights.

NOTICE

Reference to a company or product name does not imply approval or recommendation of the product by the University of California or the U.S. Energy Research & Development Administration to the exclusion of others that may be suitable.

Printed in the United States of America
Available from
National Technical Information Service
U.S. Department of Commerce
5285 Port Royal Road
Springfield, VA 22161
Price: Printed Copy $; Microfiche $3.00

Page Range	Domestic Price	Page Range	Domestic Price
001–025	$ 3.50	326–350	10.00
026–050	4.00	351–375	10.50
051–075	4.50	376–400	10.75
076–100	5.00	401–425	11.00
101–125	5.50	426–450	11.75
126–150	6.00	451–475	12.00
151–175	6.75	476–500	12.50
176–200	7.50	501–525	12.75
201–225	7.75	526–550	13.00
226–250	8.00	551–575	13.50
251–275	9.00	576–600	13.75
276–300	9.25	601–up	*
301–325	9.75		

*Add $2.50 for each additional 100 page increment from 601 to 1,000 pages; add $4.50 for each additional 100 page increment over 1,000 pages.